

A HYBRIDIZABLE DISCONTINUOUS GALERKIN METHOD FOR THE OSTROVSKY EQUATION

MUKUL DWIVEDI AND ANDREAS RUPP

ABSTRACT. This paper develops the hybridizable discontinuous Galerkin (HDG) method for the Ostrovsky equation, a nonlinear dispersive wave equation featuring both third-order dispersion and a nonlocal antiderivative term with Coriolis effect. On a bounded interval, the nonlocal operator ∂_x^{-1} is localized through an auxiliary variable v satisfying $v_x = u$ together with an additional boundary constraint that ensures uniqueness. We employ a mixed first-order formulation to decompose the dispersive operator and to localize the nonlocal term, and we couple the resulting semi-discrete HDG scheme with a θ -time stepping method for $\theta \in [1/2, 1]$. We prove L^2 -stability for suitable stabilization parameters and derive an *a priori* $L^2(\Omega)$ error estimate for smooth solutions that explicitly accounts for the nonlinear convective flux. Numerical examples illustrate the convergence properties and demonstrate the scheme's capability to handle smooth and non-smooth solutions, including solitary wave propagation and peaked solitary wave (peakon) propagation in the zero dispersive limit regime.

1. INTRODUCTION

We study the Ostrovsky equation (also known as the rotation-modified Korteweg–de Vries (KdV) equation)

$$\begin{cases} \partial_t u - \beta \partial_x^3 u + f(u)_x - \gamma \partial_x^{-1} u = 0, & x \in \mathbb{R}, t > 0, \\ u(x, 0) = u_0(x), & x \in \mathbb{R}, \end{cases} \quad (1.1)$$

where $f(u) = \frac{\alpha}{2}u^2$, u is a real valued function, $\beta \in \mathbb{R}$, $\beta \neq 0$, $\gamma > 0$ and $\alpha > 0$, and the nonlocal antiderivative term ∂_x^{-1} can be defined by $(\partial_x^{-1}g)(x) := \int_{+\infty}^x g(s) ds$, for functions g that decay as $x \rightarrow +\infty$. The Ostrovsky equation (1.1) was originally derived as an asymptotic model for weakly nonlinear long surface waves in a rotating frame of reference, where the Coriolis effect introduces a nonlocal restoring term. It was first proposed by Ostrovsky [37] in the context of oceanic wave propagation; see also [39] for additional derivations and physical discussion. The equation captures the balance between nonlinear steepening, high-frequency dispersion (when $\beta \neq 0$), and the nonlocal effect of background rotation through the term $\gamma \partial_x^{-1}u$. Here γ measures the strength of the Coriolis effect [37], while β determines the type of dispersion [18, 25, 27, 29, 50]. This nonlocal operator introduces significant mathematical and computational challenges, distinguishing (1.1) from purely local dispersive models such as the KdV equation [24], which is recovered when $\gamma = 0$. In the limit $\beta \rightarrow 0$, the equation reduces to the Ostrovsky–Hunter (OH) or Vakhnenko equation [7, 8, 9], which models short-wave perturbations in relaxing media and bubbly liquids and exhibits wave breaking and singular solitons such as peakons, cuspons, and loop solitons [17, 30, 44, 45].

The existence and stability of solitary wave solutions for the Ostrovsky equation (1.1) has been an interesting topic of research, motivated by its structural similarities with the integrable KdV and Kadomtsev–Petviashvili (KP) equations [22]. Extensive analytical and numerical investigations have been devoted to this problem in [1]. For the full dispersion case ($\beta \neq 0$), the existence and stability properties depend critically on both parameters β and γ . When $\beta > 0$, solitary waves exist for phase speeds c_w satisfying $c_w < 2\sqrt{\gamma\beta}$, with the set of ground states being stable for certain values of c_w [31]. Conversely, for $\beta < 0$, no solitary wave solutions exist when the phase speed c_w satisfies $c_w < \sqrt{140\gamma|\beta|}$ [31]. Since explicit closed-form expressions for these solitary waves are generally unavailable, numerical methods become essential for their approximation and

2020 *Mathematics Subject Classification.* 35Q53, 35G25, 65M12, 35L05.

Key words and phrases. Ostrovsky equation, HDG method, Coriolis effect, Energy stability, Error analysis.

for studying dynamical behaviors such as the persistence of a perturbed KdV soliton under the influence of weak rotation (small γ).

Analytically, the Cauchy problem for (1.1) has been extensively studied. Local and global well-posedness in the anisotropic Sobolev spaces $X_s = \{f \in H^s(\mathbb{R}) : \partial_x^{-1} f \in L^2(\mathbb{R})\}$ for $s > \frac{3}{4}$ were established by Linares and Milanes [27] using energy methods and dispersive estimates. More recent works have extended these results to lower regularity and provided refined stability analyses for solitary waves [9, 18, 47, 50, 51]. The existence and stability of solitary waves crucially depend on the sign of $\beta\gamma$: for $\beta\gamma > 0$, solitary waves exist and are stable, while for $\beta\gamma < 0$ they may be unstable or non-existent [25, 26, 29, 31]. Very recently, the spectral stability of constrained solitary waves for a generalized Ostrovsky equation, with $\beta > 0$ and $\gamma < 0$, has been investigated in [19], providing new insights into the stability properties under additional constraints. Equation (1.1) also possesses at least three conserved quantities [18], namely

$$E(u) = \int_{\mathbb{R}} u^2 dx, \quad (1.2)$$

$$V(u) = \int_{\mathbb{R}} \left(\frac{1}{3} u^3 + \frac{\gamma}{2} (\partial_x^{-1} u)^2 + \beta (\partial_x u)^2 \right) dx, \quad (1.3)$$

$$I(u) = \int_{\mathbb{R}} u dx. \quad (1.4)$$

The limit $\beta \rightarrow 0$ (convergence to the OH equation) has been rigorously justified in [26, 30], revealing a rich structure of singular traveling waves and wave breaking phenomena, and convergence of solutions in the limit ($\beta \rightarrow 0$ and $\gamma \rightarrow 0$) to the Burgers equation in [8].

Numerical approximation of the full Ostrovsky equation ($\beta \neq 0$) is particularly challenging due to the interplay of third-order dispersion, nonlinearity, and the nonlocal antiderivative term. Standard finite difference, finite element, and spectral methods often struggle to handle both the high-order derivative and the nonlocal operator simultaneously without inducing spurious oscillations or loss of stability. As noted by Kawai et al. [23], numerical methods for the full equation are still under development, and comprehensive mathematical analyses remain scarce. For the reduced Ostrovsky–Hunter equation ($\beta = 0$), several specialized schemes have been proposed, including finite difference methods [10, 40] and discontinuous Galerkin (DG) methods [52]. For the KdV equation ($\gamma = 0$), various numerical methods with extensive analysis has been studied as well, see [11, 14, 15, 20, 28] and references therein. Some numerical schemes for the Ostrovsky equation (1.1) have been developed in recent years. First finite difference scheme proposed in [21], however, the complete detail was not described to investigate solutions under both positive and negative dispersion effects. In [16], Fourier–Galerkin scheme and in [1], Fourier–pseudo-spectral scheme are used to examine the evolutions of soliton-like solutions in a periodic setting. The numerical integration of (1.1) based on its geometric structures given in [34]. Recent efforts for the full equation on a periodic domain include some conservative numerical schemes [49], a norm-conservative finite difference scheme with error estimates [23], and a geometric integration approach via the scalar auxiliary variable (SAV) method [43], both providing structure-preserving properties. The DG framework, with its flexibility in handling higher-order derivatives and nonstandard operators, offers a promising alternative. However, traditional DG methods typically result in a large number of globally coupled degrees of freedom [6], which motivates the development of more efficient alternatives such as the hybridizable discontinuous Galerkin (HDG) method.

The hybridizable discontinuous Galerkin (HDG) method, introduced by Cockburn et al. [6], addresses this issue by introducing hybrid variables on the mesh skeleton, allowing for local elimination of interior unknowns and significant reduction of the global system size. Since its inception, the HDG method has been successfully applied to a wide range of problems, including compressible flows [38], linear elasticity [46], and KdV type equations [3, 4, 11, 42]. The method has also been extended to Maxwell’s equations [2], nonlinear diffusion with internal jumps [35], the non-local Camassa–Holm–Kadomtsev–Petviashvili equation [13], and the Stokes equation with efficient multigrid solvers [33]. Recent advancements include reduced stabilization techniques [36] and localized orthogonal decomposition strategies [32], further enhancing the method’s efficiency

and applicability. Despite these developments, an HDG method for the full Ostrovsky equation (1.1) has not been previously proposed. We adopt an HDG discretization because it preserves the locality and conservation structure of DG methods while reducing globally coupled degrees of freedom to trace unknowns on the mesh skeleton via static condensation, which is particularly attractive for dispersive systems with multiple auxiliary variables [3, 6].

In this work, we develop the first high-order HDG method for the Ostrovsky equation (1.1) on a bounded interval $\Omega = (x_L, x_R)$ with appropriate boundary conditions to ensure the well posedness. We decompose the Ostrovsky equation (1.1) into the first order system by introducing auxiliary variables. The nonlocal term is localized through the auxiliary variable v by setting $v_x = u$ so that v_h approximates $\partial_x^{-1}u$, which also satisfies an additional ordinary differential equation and an additional boundary constraint is given for the uniqueness of the operator ∂_x^{-1} in a bounded domain. The signs of β and γ play a crucial role in the design of the numerical traces and the imposition of boundary conditions.

Our HDG formulation employs polynomial spaces of degree k on a one-dimensional mesh and introduces carefully designed numerical traces on element interfaces with some stabilization parameters independent of h , the mesh discretization parameter. The global HDG scheme is obtained by assembling the local formulations and imposing transmission conditions weakly. The method is shown stable and error estimates are obtained for the nonlinear flux. In particular, we derive an error estimate of order $O(h^{k+1/2})$ in the L^2 -norm for the smooth solution u . This convergence rate is typical for nonlinear dispersive equations and matches the best-known results for DG methods applied to KdV-type equations with nonlinear flux; see, e.g., [48, 52]. For HDG methods, existing analyses cover solvers for nonlinear KdV equations [42] and optimally convergent formulations for KdV-type models in linearized settings [3, 4, 11]. The present work develops a stability and error analysis for the full Ostrovsky equation (1.1), in which the nonlinear convective flux must be controlled simultaneously with a nonlocal antiderivative (Coriolis) term. This combination, together with the bounded-interval boundary constraint required for uniqueness of ∂_x^{-1} , has not been addressed in prior HDG analyses to our knowledge.

In summary, the main contributions of this paper are:

- We propose the first HDG spatial discretization for the full Ostrovsky equation (1.1), simultaneously treating the third-order dispersive term and the nonlocal antiderivative term. For time integration we employ an implicit θ -scheme where $\theta \in [\frac{1}{2}, 1]$.
- We derive a mixed first-order formulation that localizes the nonlocal operator via an auxiliary variable and incorporates boundary constraints needed to make ∂_x^{-1} well-defined on bounded domains. The resulting HDG method is efficiently implementable by static condensation: element unknowns are eliminated locally and the globally coupled system involves only single-valued trace unknowns on the mesh skeleton.
- We establish an energy stability estimate for the semi-discrete method (and its fully discrete θ -scheme counterpart) under assumptions on the stabilization parameters. Additionally, we provide the details on the error estimates of the fully discrete scheme.
- We provide an L^2 -error analysis that includes the nonlinear flux contribution, yielding the convergence bound $\|u - u_h\|_{L^2(\Omega)} = O(h^{k+1/2})$ for polynomial degree $k \geq 1$.
- Numerical tests confirm the optimal accuracy for smooth solutions and demonstrate robustness in challenging regimes, including solitary-wave propagation and non-smooth corner-type profiles, as well as the singular limit $\beta \rightarrow 0$ toward reduced OH dynamics.

Throughout, $C > 0$ denotes a generic constant independent of the mesh size h (and of Δt in fully discrete estimates), whose value may change from line to line.

The remainder of the paper is organized as follows. In Section 2 we introduce notation, meshes, and the HDG finite element spaces. Section 3 derives the mixed first-order formulation and presents the HDG spatial discretization, together with the energy stability estimate under appropriate stabilization conditions. In Section 4, we prove the semi-discrete error estimate. Section 5 analyzes the fully discrete scheme based on the implicit θ -method and establishes the corresponding stability and error bounds. Section 6 reports numerical experiments that verify the theoretical convergence rates and demonstrate robustness for solitary-wave propagation and non-smooth peaked profiles,

including the singular limit regime $\beta \rightarrow 0$. Finally, Section 7 concludes the paper and outlines possible extensions.

2. PRELIMINARIES AND NOTATION

We consider the Ostrovsky equation (1.1) on a bounded interval $\Omega = (x_L, x_R) \subset \mathbb{R}$. Let $\mathcal{T}_h = \{I_i\}_{i=1}^N$ be a partition of Ω into N subintervals $I_i = (x_{i-1}, x_i)$ with $x_0 = x_L$ and $x_N = x_R$. The mesh size is denoted by $h = \max_i |I_i|$, where $|I_i| = x_i - x_{i-1}$. We set $\mathcal{F}_h = \{x_0, x_1, \dots, x_N\}$ and $\mathcal{F}_h^0 = \{x_1, \dots, x_{N-1}\}$, and boundary points $\mathcal{F}_h^\partial = \{x_L, x_R\}$. For each element I_i , we denote its boundary by $\partial I_i = \{x_{i-1}, x_i\}$. The outward unit normal n on ∂I_i is defined as $n = -1$ at x_{i-1} and $n = 1$ at x_i .

Let $P_k(I)$ denote the space of polynomials of degree at most k on an interval I . The discontinuous polynomial space is

$$V_h^k = \{v \in L^2(\Omega) : v|_{I_i} \in P_k(I_i), \forall I_i \in \mathcal{T}_h\}.$$

The trace spaces are

$$M_h(g) = \{\hat{v} \in L^2(\mathcal{F}_h) : \hat{v}|_{\mathcal{F}_h^\partial} = g\}, \quad \widetilde{M}_h^L := L^2(\mathcal{F}_h \setminus \{x_R\}), \quad \widetilde{M}_h^R := L^2(\mathcal{F}_h \setminus \{x_L\}),$$

For $u, v \in L^2(\Omega)$, define

$$(u, v)_{I_i} = \int_{I_i} uv \, dx, \quad (u, v)_{\mathcal{T}_h} = \sum_{i=1}^N (u, v)_{I_i}, \quad \|u\|_{\mathcal{T}_h} = (u, u)_{\mathcal{T}_h}^{1/2},$$

and we set

$$\langle \varphi, \psi n \rangle_{\partial \mathcal{T}_h} = \sum_{i=1}^N \langle \varphi, \psi n \rangle_{\partial I_i} = \sum_{i=1}^N [\varphi|_{I_i}(x_i) \psi|_{I_i}(x_i) - \varphi|_{I_i}(x_{i-1}) \psi|_{I_i}(x_{i-1})],$$

for sufficiently smooth φ, ψ . The corresponding norm is $\|\varphi\|_{\partial \mathcal{T}_h} = \langle \varphi, \varphi \rangle_{\partial \mathcal{T}_h}^{1/2}$. We can also define $\langle \varphi, \psi n \rangle_{\partial \mathcal{T}_h} = \langle \varphi, \psi n \rangle_{\mathcal{I}^-} + \langle \varphi, \psi n \rangle_{\mathcal{I}^+}$, where $\langle \varphi, \psi n \rangle_{\mathcal{I}^-} = \sum_{i=1}^N \varphi|_{I_i}(x_i) \psi|_{I_i}(x_i)$ and $\langle \varphi, \psi n \rangle_{\mathcal{I}^+} = -\sum_{i=1}^N \varphi|_{I_i}(x_{i-1}) \psi|_{I_i}(x_{i-1})$.

Denote by $P : L^2(\Omega) \rightarrow P_k(\Omega)$ the standard L^2 -projection. For any function $w \in L^2(\Omega)$, we define $Pw \in V_h^k$ as the unique element satisfying

$$(Pw - w, \phi)_{I_i} = 0 \quad \forall \phi \in P_k(I_i), \forall I_i \in \mathcal{T}_h.$$

3. HDG FORMULATION FOR THE OSTROVSKY EQUATION

On $\Omega = (x_L, x_R)$ the operator ∂_x^{-1} is not uniquely defined without fixing a boundary constraint. Throughout the paper we localize the nonlocal term by introducing an auxiliary variable v such that

$$v_x = u \quad \text{in } \Omega,$$

and we impose the boundary constraint $v(x_R, t) = v_R = 0$. This choice yields a unique localization of $\partial_x^{-1}u$ on Ω and allows the Ostrovsky equation (1.1) to be rewritten as a local mixed system amenable to the HDG framework.

3.1. Mixed formulation and local boundary conditions. By introducing auxiliary variables $q := u_x$ and $p = \beta q_x$, we rewrite the Ostrovsky equation (1.1) as a first-order system

$$q = u_x, \quad p = \beta q_x, \quad v_x = u, \quad u_t - p_x + f(u)_x - \gamma v = 0, \quad (3.1)$$

along with the initial condition is $u(x, 0) = u_0(x)$ for $x \in \Omega$. We first consider the case $\beta > 0$ and we set the following boundary conditions

$$u(x_L, t) = u_L(t), \quad u(x_R, t) = u_R(t), \quad v(x_R, t) = v_R(t), \quad q(x_L, t) = q_L(t), \quad (3.2)$$

to the system (3.1). On each element I_i , the system (3.1) is a local boundary-value problem for the unknowns (u, q, p, v) . To obtain a well-posed local problem, four boundary conditions are required. We impose

$$u(x_{i-1}) = \hat{u}_{i-1}, \quad u(x_i) = \hat{u}_i, \quad v(x_i) = \hat{v}_i, \quad q(x_{i-1}) = \hat{q}_{i-1}.$$

This choice is consistent with the sign structure used in the energy estimate and yields well-posed local solvers if $\beta > 0$ and $\gamma > 0$. Given sufficiently regular initial condition and boundary data, the local problem admits a unique solution. Let (U, Q, P, V) be defined piecewise on each I_i by local solution. Then (U, Q, P, V) is a global solution of (3.1)–(3.2) in Ω if and only if it satisfy the continuity of U , Q , and $P - f(U)$ at the interior nodes $x_i \in \mathcal{F}_h^0$ together with the global boundary conditions (3.2). Thus, for these characterizations, the boundary data provided above for the local problem on I_i are the global unknowns and determined from the continuity conditions and global boundary conditions (3.2), and the system of equations for the global unknowns is square. Our HDG method mimics the above continuous structure.

3.2. HDG scheme. The local HDG formulation on I_i is: for given numerical traces on ∂I_i

$$\widehat{u}_h(x_{i-1}) =: \widehat{u}_{h,i-1}, \quad \widehat{u}_h(x_i) =: \widehat{u}_{h,i}, \quad \widehat{v}_h(x_i) =: \widehat{v}_{h,i}, \quad \widehat{q}_h(x_{i-1}) =: \widehat{q}_{h,i-1},$$

find $(u_h, v_h, p_h, q_h) \in [P_k(I_i)]^4$ such that for all test functions $(\phi_u, \phi_v, \phi_p, \phi_q) \in [P_k(I_i)]^4$, there holds

$$\begin{aligned} ((u_h)_t, \phi_u)_{I_i} + (p_h, \partial_x \phi_u)_{I_i} - (f(u_h), \partial_x \phi_u)_{I_i} - \gamma(v_h, \phi_u)_{I_i} \\ - \langle (\widehat{p}_h - \widehat{f}(u_h)) n, \phi_u \rangle_{\partial I_i} = 0, \end{aligned} \quad (3.3a)$$

$$-(v_h, \partial_x \phi_v)_{I_i} - (u_h, \phi_v)_{I_i} + \langle \widehat{v}_h n, \phi_v \rangle_{\partial I_i} = 0, \quad (3.3b)$$

$$(p_h, \phi_p)_{I_i} + \beta(q_h, \partial_x \phi_p)_{I_i} - \beta \langle \widehat{q}_h n, \phi_p \rangle_{\partial I_i} = 0, \quad (3.3c)$$

$$(q_h, \phi_q)_{I_i} + (u_h, \partial_x \phi_q)_{I_i} - \langle \widehat{u}_h n, \phi_q \rangle_{\partial I_i} = 0. \quad (3.3d)$$

The remaining numerical traces are defined as follows:

$$\begin{aligned} \widehat{v}_h &= v_h + \tau_{vq}(\widehat{q}_h - q_h)n, & \text{at } x_{i-1}, \\ \widehat{q}_h &= q_h + \tau_{qv}(\widehat{v}_h - v_h)n, & \text{at } x_i, \end{aligned} \quad (3.4)$$

$$\begin{aligned} \widehat{p}_h &= p_h + \tau_{pu}(\widehat{u}_h - u_h)n, & \text{on } \partial I_i, \\ \widehat{f}(u_h) &= f(u_h) - \tau_f(\widehat{u}_h - u_h)n, & \text{on } \partial I_i. \end{aligned} \quad (3.5)$$

The global HDG scheme is obtained by assembling the local formulations and imposing the transmission conditions weakly:

$$\langle \widehat{v}_h, \mu_v n \rangle_{\partial \mathcal{T}_h} = \langle v_R, \mu_v n \rangle_{\{x_R\}}, \quad (3.6a)$$

$$\langle \widehat{q}_h, \mu_q n \rangle_{\partial \mathcal{T}_h} = \langle q_L, \mu_q n \rangle_{\{x_L\}}, \quad (3.6b)$$

$$\langle \widehat{p}_h - \widehat{f}(u_h), \mu_p n \rangle_{\partial \mathcal{T}_h} = 0, \quad (3.6c)$$

for all $\mu_v \in \widetilde{M}_h^L$, $\mu_q \in \widetilde{M}_h^R$, and $\mu_p \in M_h(0)$. The initial condition is enforced by $u_h(\cdot, 0) = P u_0$ and the global boundary conditions

$$u_h(x_L, t) = u_L(t), \quad u_h(x_R, t) = u_R(t), \quad v_h(x_R, t) = v_R(t), \quad q_h(x_L, t) = q_L(t). \quad (3.7)$$

The globally unknown numerical traces $\widehat{u}_h \in M_h(0)$, $\widehat{v}_h \in \widetilde{M}_h^R$, and $\widehat{q}_h \in \widetilde{M}_h^L$ can be determined by solving the above weak transmission conditions (3.6). Note that, \widehat{u} is single-valued on \mathcal{F} , thus $\langle \widehat{u}_h n, \delta \rangle_{\partial \mathcal{T}_h} = 0$ for all $\delta \in M_h(0)$.

The system (3.3)–(3.6) is square. Under appropriate choices of the stabilization parameters $\tau_{vq}, \tau_{qv}, \tau_{pu}, \tau_f$, we expect unique solvability.

3.3. Stability analysis. We now establish the stability of the semi-discrete HDG scheme under the homogeneous boundary conditions $u_L(t) = u_R(t) = v_R(t) = q_L(t) = 0$. Define the discrete energy

$$\mathcal{E}_h(t) = \frac{1}{2} \|u_h(t)\|_{\mathcal{T}_h}^2.$$

To control the nonlinear term, we introduce the following stabilization function. For any oriented point $x \in \partial\mathcal{T}_h$ we set

$$\tilde{\tau}(\hat{u}_h, u_h) := \frac{1}{(\hat{u}_h - u_h)^2} \int_{\hat{u}_h}^{u_h} (f(s) - f(u_h)) n \, ds. \quad (3.8)$$

A straightforward estimate gives

$$|\tilde{\tau}(\hat{u}_h, u_h)(x)| \leq \frac{1}{2} \sup_{s \in J(\hat{u}_h(x), u_h(x))} |f'(s)|, \quad (3.9)$$

with $J(a, b) = [\min(a, b), \max(a, b)]$. In order to ensure stability, we need the point-wise inequality $\tau_f - \tilde{\tau} \geq 0$ (the first component of our collective stabilization function), for which it is sufficient to choose, e.g. $\tau_f = \sup_{s \in J(\hat{u}_h, u_h)} \frac{1}{2} |f'(s)| + \varepsilon$ for some $\varepsilon > 0$. In addition, we require the following global assumption.

Assumption 3.1 (Stabilization Parameters). *The stabilization parameters $\tau_f, \tau_{pu}, \tau_{vq}, \tau_{qv}$ are chosen such that the following inequalities hold pointwise on $\partial\mathcal{T}_h$:*

$$\tau_f - \tilde{\tau} \geq \tilde{C}, \quad \tau_{pu} \geq c, \quad \frac{\beta}{2} - \frac{\gamma}{2} \tau_{vq}^2 \geq c, \quad \frac{\gamma}{2} - \frac{\beta}{2} \tau_{qv}^2 \geq c.$$

Here, \tilde{C} is chosen sufficiently large, and $c > 0$ is chosen such that $c - \tilde{C}\delta \geq 0$, where \tilde{C} is a constant arising in the proof of Theorem 4.3 and $\delta > 0$ is a small parameter from Young's inequality. For the stability statement alone it suffices to take $\tilde{C} = c = 0$.

Theorem 3.2 (Stability). *Under the homogeneous boundary conditions stated above and Assumption 3.1, the solution of the HDG scheme (3.3) satisfies*

$$\frac{d}{dt} \mathcal{E}_h(t) \leq 0.$$

Proof. We begin by choosing the test functions

$$\phi_u = u_h, \quad \phi_v = -\gamma v_h, \quad \phi_p = -q_h, \quad \phi_q = p_h,$$

in the global equations (3.3a)–(3.3d), adding these four equations and summing on all I_i yields

$$\begin{aligned} \frac{1}{2} \frac{d}{dt} \|u_h\|_{\mathcal{T}_h}^2 + (p_h, \partial_x u_h)_{\mathcal{T}_h} + (u_h, \partial_x p_h)_{\mathcal{T}_h} - \langle \hat{p}_h, u_h n \rangle_{\partial\mathcal{T}_h} - \langle \hat{u}_h, p_h n \rangle_{\partial\mathcal{T}_h} \\ - (f(u_h), \partial_x u_h)_{\mathcal{T}_h} + \langle \widehat{f(u_h)}, u_h n \rangle_{\partial\mathcal{T}_h} + \gamma(v_h, \partial_x v_h)_{\mathcal{T}_h} - \gamma \langle \hat{v}_h, v_h n \rangle_{\partial\mathcal{T}_h} \\ - \beta(q_h, \partial_x q_h)_{\mathcal{T}_h} + \beta \langle \hat{q}_h, q_h n \rangle_{\partial\mathcal{T}_h} = 0. \end{aligned}$$

Using integration by parts and the transmission conditions (3.6) we obtain the identity

$$\begin{aligned} \frac{1}{2} \frac{d}{dt} \|u_h\|_{\mathcal{T}_h}^2 + \langle (\hat{p}_h - p_h), (\hat{u}_h - u_h) n \rangle_{\partial\mathcal{T}_h} - (f(u_h), \partial_x u_h)_{\mathcal{T}_h} - \langle \widehat{f(u_h)}, (\hat{u}_h - u_h) n \rangle_{\partial\mathcal{T}_h} \\ - \frac{\gamma}{2} (-\hat{v}_h(x_L)^2 + \hat{v}_h(x_R)^2) + \frac{\gamma}{2} \langle (\hat{v}_h - v_h)^2, n \rangle_{\partial\mathcal{T}_h} \\ + \frac{\beta}{2} (-\hat{q}_h(x_L)^2 + \hat{q}_h(x_R)^2) - \frac{\beta}{2} \langle (\hat{q}_h - q_h)^2, n \rangle_{\partial\mathcal{T}_h} = 0. \end{aligned}$$

Let G be an antiderivative of f . Then

$$(f(u_h), \partial_x u_h)_{\mathcal{T}_h} = \langle G(u_h), n \rangle_{\partial\mathcal{T}_h} = \left\langle \int_{\hat{u}_h}^{u_h} f(s) \, ds, n \right\rangle_{\partial\mathcal{T}_h}.$$

Combining this with the definition of $\widehat{f(u_h)}$ from (3.5), we have

$$\begin{aligned} & - (f(u_h), \partial_x u_h)_{\mathcal{T}_h} - \langle \widehat{f(u_h)}, (\hat{u}_h - u_h) n \rangle_{\partial\mathcal{T}_h} \\ & = - \left\langle \int_{\hat{u}_h}^{u_h} (f(s) - f(u_h)) \, ds, n \right\rangle_{\partial\mathcal{T}_h} - \langle (\widehat{f(u_h)} - f(u_h)), (\hat{u}_h - u_h) n \rangle_{\partial\mathcal{T}_h} \\ & = \langle (\tau_f - \tilde{\tau})(\hat{u}_h - u_h)^2, 1 \rangle_{\partial\mathcal{T}_h}. \end{aligned}$$

where $\tilde{\tau}$ is defined by (3.9). We insert the definitions of the numerical traces $\hat{p}_h, \hat{v}_h, \hat{q}_h$ from (3.4)-(3.5) and apply the boundary conditions, which gives

$$\begin{aligned} & \frac{1}{2} \frac{d}{dt} \|u_h\|_{\mathcal{T}_h}^2 + \tau_{pu} \langle (\hat{u}_h - u_h)^2, 1 \rangle_{\partial\mathcal{T}_h} + \langle \tau_f - \tilde{\tau}, (\hat{u}_h - u_h)^2 \rangle_{\partial\mathcal{T}_h} \\ & + \frac{\gamma}{2} \hat{v}_h(x_L)^2 + \frac{\gamma}{2} \tau_{vq}^2 \langle (\hat{q}_h - q_h)^2, n \rangle_{\mathcal{I}^+} + \frac{\gamma}{2} \langle (\hat{v}_h - v_h)^2, n \rangle_{\mathcal{I}^-} \\ & + \frac{\beta}{2} \hat{q}_h(x_R)^2 - \frac{\beta}{2} \langle (\hat{q}_h - q_h)^2, n \rangle_{\mathcal{I}^+} - \frac{\beta}{2} \tau_{qv}^2 \langle (\hat{v}_h - v_h)^2, n \rangle_{\mathcal{I}^-} = 0. \end{aligned} \quad (3.10)$$

Applying assumption 3.1 implies

$$\frac{1}{2} \frac{d}{dt} \|u_h\|_{\mathcal{T}_h}^2 \leq 0.$$

This completes the proof. \square

Remark 3.3 (Conservative property for periodic problems with $\beta > 0$ and $\gamma > 0$). *For periodic boundary conditions ($\hat{v}_h(x_L) = \hat{v}_h(x_R)$, $\hat{q}_h(x_L) = \hat{q}_h(x_R)$, and $\hat{u}_h(x_L) = \hat{u}_h(x_R)$), our HDG scheme (3.3)-(3.6) can be made exactly conservative by an appropriate choice of the stabilization parameters. As we mentioned in Assumption 3.1 that we can take $\tilde{C} = c = 0$ for the stability analysis. Therefore, by setting $\tau_{pu} = 0$, $\tau_{vq} = \sqrt{\beta/\gamma}$, $\tau_{qv} = \sqrt{\gamma/\beta}$, and $\tau_f = \tilde{\tau}$ (pointwise), (3.10) yields*

$$\frac{1}{2} \frac{d}{dt} \|u_h\|_{\mathcal{T}_h}^2 = 0,$$

making the scheme energy-conservative.

In practice we take $\tau_f = \tilde{\tau}$, where $\tilde{\tau}$ is evaluated elementwise from the current trace and if $\hat{u}_h = u_h$ at a quadrature point, we interpret the quotient-based definition of $\tilde{\tau}$ in the limiting sense (equivalently, by replacing the quotient with $|f'(u_h)|$), which is well-defined for the smooth fluxes considered here.

Remark 3.4 (Case $\beta < 0$). *The stability analysis and numerical traces presented above assume $\beta > 0$. For the case $\beta < 0$, the stability analysis requires a different choice of numerical traces and boundary conditions for the auxiliary variable q . Specifically, we now set local given traces on ∂I_i as*

$$\hat{u}_h(x_{i-1}) =: \hat{u}_{h,i-1}, \quad \hat{u}_h(x_i) =: \hat{u}_{h,i}, \quad \hat{v}_h(x_i) =: \hat{v}_{h,i}, \quad \hat{q}_h(x_i) =: \hat{q}_{h,i},$$

and impose the global boundary condition $u(x_L, t) = u_L(t)$, $u(x_R, t) = u_R(t)$, $v(x_R, t) = v_R(t)$, and $q(x_R, t) = q_R(t)$. The remaining local numerical traces are accordingly modified to

$$\hat{v}_h = v_h \quad \text{and} \quad \hat{q}_h = q_h, \quad \text{at } x_{i-1},$$

along with other numerical traces (3.5), while the transmission condition for q becomes

$$\langle \hat{q}_h, \mu_q n \rangle_{\partial\mathcal{T}_h} = \langle q_R, \mu_q n \rangle_{\{x_R\}}.$$

Proceeding with the same energy argument as in the proof of Theorem 3.2, the energy identity (3.10) becomes

$$\begin{aligned} & \frac{1}{2} \frac{d}{dt} \|u_h\|_{\mathcal{T}_h}^2 + \tau_{pu} \langle (\hat{u}_h - u_h)^2, 1 \rangle_{\partial\mathcal{T}_h} + \langle \tau_f - \tilde{\tau}, (\hat{u}_h - u_h)^2 \rangle_{\partial\mathcal{T}_h} \\ & + \frac{\gamma}{2} \hat{v}_h(x_L)^2 + \frac{\gamma}{2} \langle (\hat{v}_h - v_h)^2, n \rangle_{\mathcal{I}^-} - \frac{\beta}{2} \hat{q}_h(x_L)^2 - \frac{\beta}{2} \langle (\hat{q}_h - q_h)^2, n \rangle_{\mathcal{I}^-} = 0. \end{aligned}$$

Under the same homogeneous boundary conditions, stability is ensured if the stabilization parameters satisfy $\tau_f - \tilde{\tau} \geq \tilde{C}$, $\tau_{pu} \geq c$, with $\tilde{C} \geq 0$ and $c \geq 0$ as in Assumption 3.1.

4. ERROR ANALYSIS

We now present an error analysis for the proposed HDG method (3.3). The analysis is based on standard L^2 projections and follows the usual approach for error estimation of discontinuous Galerkin methods. Let (u, v, p, q) denote the exact solution of the OV equation (1.1) with sufficient regularity, and let (u_h, v_h, p_h, q_h) be the semi-discrete HDG approximation defined by (3.3).

We begin by considering the L^2 projection onto the local polynomial space $P_k(I_i)$.

Lemma 4.1 (Inverse inequalities [5, 48]). *For every $v_h \in V_h^k$ ($k \geq 0$), there exists a positive constant C independent of v_h and h , such that the following estimates hold*

$$\|\partial_x v_h\|_{\mathcal{T}_h} \leq Ch^{-1}\|v_h\|_{\mathcal{T}_h}, \quad \|v_h\|_{\partial\mathcal{T}_h} \leq Ch^{-\frac{1}{2}}\|v_h\|_{\mathcal{T}_h}, \quad \|v_h\|_{L^\infty(\mathcal{T}_h)} \leq Ch^{-\frac{1}{2}}\|v_h\|_{\mathcal{T}_h}. \quad (4.1)$$

Lemma 4.2 (Interpolation inequality [5, 48]). *For any $\omega \in H^{k+1}(\mathcal{T}_h)$ there exists a constant $C > 0$, independent of h , such that*

$$\|P\omega - \omega\|_{\mathcal{T}_h} + h^{\frac{1}{2}}\|P\omega - \omega\|_{L^\infty(\mathcal{T}_h)} + h^{\frac{1}{2}}\|P\omega - \omega\|_{\partial\mathcal{T}_h} \leq Ch^{k+1}. \quad (4.2)$$

To deal with the nonlinear flux, we make an *a priori* assumption, that for all $t < T$ and small enough h , there holds

$$\|u - u_h\|_{\mathcal{T}_h} \leq h. \quad (4.3)$$

Consequently, we have

$$\|u - u_h\|_{L^\infty(\mathcal{T}_h)} \leq Ch^{1/2}. \quad (4.4)$$

The above assumption is not required for linear flux $f(u) = cu$.

We decompose the errors into projection errors and the errors between the projections and the numerical solutions

$$e_\omega := \omega - \omega_h = (P\omega - \omega_h) - (P\omega - \omega) =: \xi^\omega - \rho^\omega, \quad \omega \in \{u, v, p, q\}.$$

On the skeleton $\partial\mathcal{T}_h$, we introduce

$$\widehat{\xi}^u := u - \widehat{u}_h, \quad \widehat{\xi}^q := q - \widehat{q}_h, \quad \widehat{\xi}^p := p - \widehat{p}_h, \quad \widehat{\xi}^v := v - \widehat{v}_h, \quad (4.5)$$

so that the simple algebraic manipulations and definitions (3.4)-(3.5) imply that in I_i

$$\begin{aligned} \widehat{\xi}^v &= \xi^v + \tau_{vq}(\widehat{\xi}^q - \xi^q)n - (\rho^v - \tau_{vq}\rho^q)n, & \text{at } x_{i-1}, \\ \widehat{\xi}^q &= \xi^q + \tau_{qv}(\widehat{\xi}^v - \xi^v)n - (\rho^q - \tau_{qv}\rho^v)n, & \text{at } x_i, \end{aligned} \quad (4.6)$$

and

$$\widehat{\xi}^p = \xi^p + \tau_{pu}(\widehat{\xi}^u - \xi^u)n - (\rho^p - \tau_{pu}\rho^u)n, \quad \text{at } x_{i-1} \text{ and } x_i, \quad (4.7)$$

Since the exact solution satisfies (3.3)-(3.6), the HDG scheme (3.3) yields the error equations

$$\begin{aligned} ((e_u)_t, \phi_u)_{\mathcal{T}_h} + (e_p, \partial_x \phi_u)_{\mathcal{T}_h} - (f(u) - f(u_h), \partial_x \phi_u)_{\mathcal{T}_h} - \gamma(e_v, \phi_u)_{\mathcal{T}_h} \\ - \langle (p - \widehat{p}_h) - (f(u) - \widehat{f}(u_h)), \phi_u n \rangle_{\partial\mathcal{T}_h} = 0, \end{aligned} \quad (4.8a)$$

$$-(e_v, \partial_x \phi_v)_{\mathcal{T}_h} - (e_u, \phi_v)_{\mathcal{T}_h} + \langle v - \widehat{v}_h, \phi_v n \rangle_{\partial\mathcal{T}_h} = 0, \quad (4.8b)$$

$$(e_p, \phi_p)_{\mathcal{T}_h} + \beta(e_q, \partial_x \phi_p)_{\mathcal{T}_h} - \beta(q - \widehat{q}_h, \phi_p n)_{\partial\mathcal{T}_h} = 0, \quad (4.8c)$$

$$(e_q, \phi_q)_{\mathcal{T}_h} + (e_u, \partial_x \phi_q)_{\mathcal{T}_h} - \langle u - \widehat{u}_h, \phi_q n \rangle_{\partial\mathcal{T}_h} = 0. \quad (4.8d)$$

Using the decomposition $e_\omega = \xi^\omega - \rho^\omega$ ($\omega \in \{u, q, p, v\}$), definition on L^2 projection ρ^ω and (4.5), we obtain the error equations in terms of ξ and ρ :

$$\begin{aligned} ((\xi^u)_t, \phi_u)_{\mathcal{T}_h} + (\xi^p, \partial_x \phi_u)_{\mathcal{T}_h} - (f(u) - f(u_h), \partial_x \phi_u)_{\mathcal{T}_h} - \gamma(\xi^v, \phi_u)_{\mathcal{T}_h} \\ - \langle \widehat{\xi}^p, \phi_u n \rangle_{\partial\mathcal{T}_h} + \langle (f(u) - \widehat{f}(u_h)), \phi_u n \rangle_{\partial\mathcal{T}_h} = 0 \end{aligned} \quad (4.9a)$$

$$- (\xi^v, \partial_x \phi_v)_{\mathcal{T}_h} - (\xi^u, \phi_v)_{\mathcal{T}_h} + \langle \widehat{\xi}^v, \phi_v n \rangle_{\partial\mathcal{T}_h} = 0, \quad (4.9b)$$

$$(\xi^p, \phi_p)_{\mathcal{T}_h} + \beta(\xi^q, \partial_x \phi_p)_{\mathcal{T}_h} - \beta(\widehat{\xi}^q, \phi_p n)_{\partial\mathcal{T}_h} = 0, \quad (4.9c)$$

$$(\xi^q, \phi_q)_{\mathcal{T}_h} + (\xi^u, \partial_x \phi_q)_{\mathcal{T}_h} - \langle \widehat{\xi}^u, \phi_q n \rangle_{\partial\mathcal{T}_h} = 0, \quad (4.9d)$$

and transmission condition (3.6) and smoothness of exact solution (u, v, p, q) gives

$$\langle \widehat{\xi}^v, \mu_v n \rangle_{\partial\mathcal{T}_h} = 0, \quad \langle \widehat{\xi}^q, \mu_q n \rangle_{\partial\mathcal{T}_h} = 0, \quad \langle \widehat{\xi}^p - (f(u) - \widehat{f}(u_h)), \mu_p n \rangle_{\partial\mathcal{T}_h} = 0, \quad (4.10a)$$

for all $\mu_v \in \widetilde{M}_h^L$, $\mu_q \in \widetilde{M}_h^R$, and $\mu_p \in M_h(0)$. These equations form the starting point for the subsequent error estimates. We now state and prove the main error estimate. We assume that the exact solution (u, v, p, q) is sufficiently smooth, specifically that each component belongs to $H^{k+1}(\Omega)$ for the spatial regularity and is continuously differentiable in time.

Theorem 4.3. *Under the above smoothness assumptions on exact tuple solution (u, v, p, q) and with the stabilization parameters chosen according to Assumption 3.1, the error between the exact solution and the semi-discrete HDG solution (u_h, v_h, p_h, q_h) satisfies*

$$\|u - u_h\|_{L^2(\Omega)} \leq Ch^{k+1/2}, \quad k \geq 1, \quad (4.11)$$

provided h is sufficiently small, where constant C may depend on the exact solution, the polynomial degree k , the parameters β, γ , the final time T , and the mesh regularity, but is independent of the mesh size h .

Proof. We follow the energy argument used in the stability analysis. Choose the test functions in (4.9) as

$$\phi_u = \xi^u, \quad \phi_v = -\gamma \xi^v, \quad \phi_p = -\xi^q, \quad \phi_q = \xi^p.$$

Adding the four equations (4.9a)–(4.9d) with these test functions and integration by parts yields

$$\begin{aligned} \frac{1}{2} \frac{d}{dt} \|\xi^u\|_{\mathcal{T}_h}^2 + \langle \xi^p, \xi^u n \rangle_{\partial\mathcal{T}_h} - \langle \widehat{\xi}^p, \xi^u n \rangle_{\partial\mathcal{T}_h} - \langle \widehat{\xi}^u, \xi^p n \rangle_{\partial\mathcal{T}_h} + \frac{\gamma}{2} \langle \xi^v, \xi^v n \rangle_{\partial\mathcal{T}_h} - \gamma \langle \widehat{\xi}^v, \xi^v n \rangle_{\partial\mathcal{T}_h} \\ - \frac{\beta}{2} \langle \xi^q, \xi^q n \rangle_{\partial\mathcal{T}_h} + \beta \langle \widehat{\xi}^q, \xi^q n \rangle_{\partial\mathcal{T}_h} = (f(u) - f(u_h), \partial_x \xi^u)_{\mathcal{T}_h} - \langle f(u) - \widehat{f}(u_h), \xi^u n \rangle_{\partial\mathcal{T}_h}. \end{aligned}$$

Now using the conditions (4.10), we obtain

$$\begin{aligned} \frac{1}{2} \frac{d}{dt} \|\xi^u\|_{\mathcal{T}_h}^2 + \langle (\widehat{\xi}^p - \xi^p), (\widehat{\xi}^u - \xi^u) n \rangle_{\partial\mathcal{T}_h} + \frac{\gamma}{2} \widehat{\xi}^v (x_L)^2 + \frac{\gamma}{2} \langle (\widehat{\xi}^v - \xi^v)^2, n \rangle_{\partial\mathcal{T}_h} \\ + \frac{\beta}{2} \widehat{\xi}^q (x_R)^2 - \frac{\beta}{2} \langle (\widehat{\xi}^q - \xi^q)^2, n \rangle_{\partial\mathcal{T}_h} = (f(u) - f(u_h), \partial_x \xi^u)_{\mathcal{T}_h} + \langle f(u) - \widehat{f}(u_h), (\widehat{\xi}^u - \xi^u) n \rangle_{\partial\mathcal{T}_h}. \end{aligned}$$

Utilizing definitions of traces (4.6)–(4.7) and (3.5), we get

$$\begin{aligned} \frac{1}{2} \frac{d}{dt} \|\xi^u\|_{\mathcal{T}_h}^2 + \tau_{pu} \langle (\widehat{\xi}^u - \xi^u)^2, 1 \rangle_{\partial\mathcal{T}_h} + \frac{\gamma}{2} \widehat{\xi}^v (x_L)^2 + \frac{\gamma}{2} \langle (\widehat{\xi}^v - \xi^v)^2, n \rangle_{\mathcal{I}^-} + \frac{\gamma}{2} \tau_{vq}^2 \langle (\widehat{\xi}^q - \xi^q)^2, n \rangle_{\mathcal{I}^+} \\ + \frac{\beta}{2} \widehat{\xi}^q (x_R)^2 - \frac{\beta}{2} \langle (\widehat{\xi}^q - \xi^q)^2, n \rangle_{\mathcal{I}^+} - \frac{\beta}{2} \tau_{qv}^2 \langle (\widehat{\xi}^v - \xi^v)^2, n \rangle_{\mathcal{I}^-} \\ = (f(u) - f(u_h), \partial_x \xi^u)_{\mathcal{T}_h} + \langle f(u) - f(u_h), (\widehat{\xi}^u - \xi^u) n \rangle_{\partial\mathcal{T}_h} + \langle \tau_f (\widehat{u}_h - u_h), (\widehat{\xi}^u - \xi^u) \rangle_{\partial\mathcal{T}_h} \\ + \langle (\rho^p - \tau_{pu} \rho^u n), (\widehat{\xi}^u - \xi^u) n \rangle_{\partial\mathcal{T}_h} + \frac{\beta}{2} \langle (\rho^q - \tau_{qv} \rho^v)^2, n \rangle_{\mathcal{I}^-} - \frac{\gamma}{2} \langle (\rho^v - \tau_{vq} \rho^q)^2, n \rangle_{\mathcal{I}^+} \\ - \beta \langle (\rho^q - \tau_{qv} \rho^v), \tau_{qv} (\widehat{\xi}^v - \xi^v) n \rangle_{\mathcal{I}^-} + \gamma \langle (\rho^v - \tau_{vq} \rho^q), \tau_{vq} (\widehat{\xi}^q - \xi^q) n \rangle_{\mathcal{I}^+}. \end{aligned}$$

Employing the Assumption 3.1 and ignoring some positive terms from the left hand side, we have

$$\begin{aligned} \frac{1}{2} \frac{d}{dt} \|\xi^u\|_{\mathcal{T}_h}^2 + c(\|\widehat{\xi}^u - \xi^u\|_{\partial\mathcal{T}_h}^2 + \|\widehat{\xi}^q - \xi^q\|_{\mathcal{I}^-}^2 + \|\widehat{\xi}^v - \xi^v\|_{\mathcal{I}^+}^2) \leq (f(u) - f(u_h), \partial_x \xi^u)_{\mathcal{T}_h} \\ + \langle f(u) - f(u_h), (\widehat{\xi}^u - \xi^u) n \rangle_{\partial\mathcal{T}_h} - \langle \tau_f (\widehat{\xi}^u - \xi^u + \rho^u), (\widehat{\xi}^u - \xi^u) \rangle_{\partial\mathcal{T}_h} \\ + \langle (\rho^p - \tau_{pu} \rho^u n), (\widehat{\xi}^u - \xi^u) n \rangle_{\partial\mathcal{T}_h} + \frac{\beta}{2} \langle (\rho^q - \tau_{qv} \rho^v)^2, n \rangle_{\mathcal{I}^-} - \frac{\gamma}{2} \langle (\rho^v - \tau_{vq} \rho^q)^2, n \rangle_{\mathcal{I}^+} \\ - \beta \langle (\rho^q - \tau_{qv} \rho^v), \tau_{qv} (\widehat{\xi}^v - \xi^v) n \rangle_{\mathcal{I}^-} + \gamma \langle (\rho^v - \tau_{vq} \rho^q), \tau_{vq} (\widehat{\xi}^q - \xi^q) n \rangle_{\mathcal{I}^+}. \end{aligned} \quad (4.12)$$

Now we estimate the right hand side using the Taylor's expansion, projection estimates, and trace definition (3.5). We write

$$f(u) - f(u_h) = f'(u)(u - u_h) - \frac{1}{2} f''_u (u - u_h)^2 = f'(u)(\xi^u - \rho^u) - \frac{1}{2} f''_u (\xi^u - \rho^u)^2,$$

so that the nonlinear part of the right hand side of the inequality (4.12) becomes

$$\begin{aligned}
& (f(u) - f(u_h), \partial_x \xi^u)_{\mathcal{T}_h} + \langle f(u) - f(u_h), (\widehat{\xi}^u - \xi^u)n \rangle_{\partial \mathcal{T}_h} - \langle \tau_f(\widehat{\xi}^u - \xi^u + \rho^u), (\widehat{\xi}^u - \xi^u) \rangle_{\partial \mathcal{T}_h} \\
&= \underbrace{(f'(u)(\xi^u - \rho^u), \partial_x \xi^u)_{\mathcal{T}_h} + \langle f'(u)(\xi^u - \rho^u), n(\widehat{\xi}^u - \xi^u) \rangle_{\partial \mathcal{T}_h}}_{f_1} \\
&\quad - \underbrace{\left(\frac{1}{2} f''_u (\xi^u - \rho^u)^2, \partial_x \xi^u \right)_{\mathcal{T}_h} - \left\langle \frac{1}{2} f''_u (\xi^u - \rho^u)^2, n(\widehat{\xi}^u - \xi^u) \right\rangle_{\partial \mathcal{T}_h}}_{f_2} \\
&\quad - \underbrace{\langle \tau_f(\widehat{\xi}^u - \xi^u + \rho^u), (\widehat{\xi}^u - \xi^u) \rangle_{\partial \mathcal{T}_h}}_{f_3}.
\end{aligned} \tag{4.13}$$

Incorporating interpolation (4.2) and inverse inequalities (4.1), integration by parts, Young's inequality, and an *a priori* assumption (4.3) with $|u - \bar{u}|_{I_i} = \mathcal{O}(h)$ on each I_i for some constant \bar{u} , we have

$$\begin{aligned}
f_1 &= (f'(u)(\xi^u - \rho^u), \partial_x \xi^u)_{\mathcal{T}_h} + \langle f'(u)(\xi^u - \rho^u), n(\widehat{\xi}^u - \xi^u) \rangle_{\partial \mathcal{T}_h} \\
&= \left(f'(u), \frac{1}{2} \partial_x (\xi^u)^2 \right)_{\mathcal{T}_h} - (f'(u)\rho^u, \partial_x \xi^u)_{\mathcal{T}_h} + \langle f'(u)(\xi^u - \rho^u), n(\widehat{\xi}^u - \xi^u) \rangle_{\partial \mathcal{T}_h} \\
&= - \left(f''(u)u_x, \frac{1}{2} (\xi^u)^2 \right)_{\mathcal{T}_h} + \left\langle (f'(u) - f'(\bar{u})), n \frac{1}{2} (\xi^u)^2 \right\rangle_{\partial \mathcal{T}_h} + \left\langle f'(\bar{u}), n \frac{1}{2} (\xi^u)^2 \right\rangle_{\partial \mathcal{T}_h} \\
&\quad - \left((f'(u) - f'(\bar{u}))\rho^u, \partial_x \xi^u \right)_{\mathcal{T}_h} + \langle (f'(u) - f'(\bar{u}))(\xi^u - \rho^u), n(\widehat{\xi}^u - \xi^u) \rangle_{\partial \mathcal{T}_h} \\
&\quad + \langle f'(\bar{u})(\xi^u - \rho^u), n(\widehat{\xi}^u - \xi^u) \rangle_{\partial \mathcal{T}_h} - \left\langle f'(\bar{u}), n \frac{1}{2} (\widehat{\xi}^u)^2 \right\rangle_{\partial \mathcal{T}_h} \\
&\leq C \|f''(u)\|_{L^\infty(\mathcal{T}_h)} \|u_x\|_{L^\infty(\mathcal{T}_h)} \|\xi^u\|_{\mathcal{T}_h}^2 + Ch^{-\frac{1}{2}} |f'(u) - f'(\bar{u})|_{\partial \mathcal{T}_h} \|\xi^u\|_{\mathcal{T}_h}^2 \\
&\quad - \left\langle f'(\bar{u}), n \frac{1}{2} (\xi^u)^2 \right\rangle_{\partial \mathcal{T}_h} - \left\langle f'(\bar{u}), n \frac{1}{2} (\widehat{\xi}^u)^2 \right\rangle_{\partial \mathcal{T}_h} + \langle f'(\bar{u})\xi^u, n\widehat{\xi}^u \rangle_{\partial \mathcal{T}_h} \\
&\quad + h^{-1} |f'(u) - f'(\bar{u})|_{\mathcal{T}_h} \|\rho^u\|_{\mathcal{T}_h} \|\xi^u\|_{\mathcal{T}_h} \\
&\quad + h^{-\frac{1}{2}} |f'(u) - f'(\bar{u})|_{\partial \mathcal{T}_h} (\|\rho^u\|_{\mathcal{T}_h} + \|\xi^u\|_{\mathcal{T}_h}) \|\widehat{\xi}^u - \xi^u\|_{\partial \mathcal{T}_h} - \langle f'(\bar{u})\rho^u, n(\widehat{\xi}^u - \xi^u) \rangle_{\partial \mathcal{T}_h} \\
&\leq C(\delta) \|\xi^u\|_{\mathcal{T}_h}^2 + \frac{1}{2} |f'(\bar{u})| \|\widehat{\xi}^u - \xi^u\|_{\partial \mathcal{T}_h}^2 + Ch^{2k+1} + C \|\widehat{\xi}^u - \xi^u\|_{\partial \mathcal{T}_h}^2, \\
f_2 &= - \left(\frac{1}{2} f''_u (\xi^u - \rho^u)^2, \partial_x \xi^u \right)_{\mathcal{T}_h} - \left\langle \frac{1}{2} f''_u (\xi^u - \rho^u)^2, n(\widehat{\xi}^u - \xi^u) \right\rangle_{\partial \mathcal{T}_h} \\
&\leq Ch^{-1} |u - u_h|_{\mathcal{T}_h} \|\xi^u - \rho^u\|_{\mathcal{T}_h} \|\xi^u\|_{\mathcal{T}_h} + Ch^{-\frac{1}{2}} |u - u_h|_{\partial \mathcal{T}_h} \|\xi^u - \rho^u\|_{\mathcal{T}_h} \|\widehat{\xi}^u - \xi^u\|_{\partial \mathcal{T}_h} \\
&\leq Ch^{2k+2} + C \|\xi^u\|_{\mathcal{T}_h}^2 + C \|\widehat{\xi}^u - \xi^u\|_{\partial \mathcal{T}_h}^2, \\
f_3 &= - \langle \tau_f(\widehat{\xi}^u - \xi^u + \rho^u), (\widehat{\xi}^u - \xi^u) \rangle_{\partial \mathcal{T}_h} = - \langle \tau_f, (\widehat{\xi}^u - \xi^u)^2 \rangle_{\partial \mathcal{T}_h} - \langle \tau_f \rho^u, (\widehat{\xi}^u - \xi^u) \rangle_{\partial \mathcal{T}_h}.
\end{aligned}$$

Hence, substituting the values of f_i 's into the equation (4.13) and employing the Young's inequality, we have

$$f_1 + f_2 + f_3 \leq - \left\langle \tau_f - \frac{1}{2} |f'(\bar{u})|, (\widehat{\xi}^u - \xi^u)^2 \right\rangle_{\partial \mathcal{T}_h} + C(\delta) h^{2k+1} + C \|\xi^u\|_{\mathcal{T}_h}^2 + \frac{\bar{C}\delta}{2} \|\widehat{\xi}^u - \xi^u\|_{\partial \mathcal{T}_h}^2. \tag{4.14}$$

The remaining parts of (4.12) estimated using Young's inequality and projections estimates (4.2). Thus we have

$$\begin{aligned}
& \langle (\rho^p - \tau_{pu}\rho^u n), (\widehat{\xi}^u - \xi^u)n \rangle_{\partial \mathcal{T}_h} + \frac{\beta}{2} \langle (\rho^q - \tau_{qv}\rho^v)^2, n \rangle_{\mathcal{I}^-} - \frac{\gamma}{2} \langle (\rho^v - \tau_{vq}\rho^q)^2, n \rangle_{\mathcal{I}^+} \\
&\quad - \beta \langle (\rho^q - \tau_{qv}\rho^v), \tau_{qv}(\widehat{\xi}^v - \xi^v)n \rangle_{\mathcal{I}^-} + \gamma \langle (\rho^v - \tau_{vq}\rho^q), \tau_{vq}(\widehat{\xi}^q - \xi^q)n \rangle_{\mathcal{I}^+} \\
&\leq Ch^{2k+1} + \frac{\bar{C}\delta}{2} \|\widehat{\xi}^u - \xi^u\|_{\partial \mathcal{T}_h}^2 + \bar{C}\delta (\|\widehat{\xi}^q - \xi^q\|_{\mathcal{I}^-}^2 + \|\widehat{\xi}^v - \xi^v\|_{\mathcal{I}^+}^2).
\end{aligned} \tag{4.15}$$

Since we have $-(\tau_f - \frac{1}{2}|f'(c)|) \leq 0$ and $c - \bar{C}\delta \geq 0$ from Assumption 3.1, therefore, estimates (4.12), (4.14), and (4.15) together gives

$$\frac{1}{2} \frac{d}{dt} \|\xi^u\|_{\mathcal{T}_h}^2 \leq Ch^{2k+1} + C\|\xi^u\|_{\mathcal{T}_h}^2, \quad (4.16)$$

where δ can be taken small as it comes from the application of the Young's inequality and we have ignored the positive terms from the left hand side. The generic constants C and \bar{C} are positive and independent from h . Applying the Gronwall's inequality, and using the fact that $\xi^u(0) = 0$ (because $u_h(\cdot, 0) = Pu_0$), we obtain

$$\|\xi^u(t)\|_{\mathcal{T}_h}^2 \leq Ch^{2k+1}, \quad 0 \leq t \leq T.$$

Finally, by the triangle inequality and projection estimate (4.2), we obtain

$$\|u - u_h\|_{\mathcal{T}_h} \leq \|\xi^u\|_{\mathcal{T}_h} + \|\rho^u\|_{\mathcal{T}_h} \leq Ch^{k+1/2},$$

which completes the proof. \square

It remains to justify an *a priori* assumption (4.3). The justification of assumption (4.3) follows via a continuity argument [48]. For $k \geq 1$ and h sufficiently small, $Ch^{k+1/2} < \frac{1}{2}h$, where C is constant in (4.11) can be exactly determined by using the final time T . Define $t^* := \sup\{t : \|u(t) - u_h(t)\|_{\mathcal{T}_h} \leq h^2\}$. Initial conditions satisfy $t^* > 0$ by projection properties. Assume $t^* < T$. Continuity implies $\|u(t^*) - u_h(t^*)\|_{\mathcal{T}_h} = h$. Theorem 4.3 (valid for $t \leq t^*$ under the assumption) yields

$$\|u(t^*) - u_h(t^*)\|_{\mathcal{T}_h} \leq Ch^{k+1/2} < \frac{1}{2}h.$$

This contradicts the equality if $t^* < T$, and hence $t^* \geq T$. The consequences in (4.4) follow from inverse and interpolation inequalities (4.1), and (4.3).

5. TIME DISCRETIZATION

We discretize the semi-discrete HDG formulation (3.3)–(3.6) in time by an implicit θ -method. Let $\Delta t > 0$ be a fixed time step, $t_n := n\Delta t$, and denote by $(u_h^n, v_h^n, p_h^n, q_h^n)$ and by the hybrid variables $(\hat{u}_h^n, \hat{v}_h^n, \hat{q}_h^n)$ the approximations at time t_n . We introduce the standard difference quotient

$$\delta_t u_h^{n+1} := \frac{u_h^{n+1} - u_h^n}{\Delta t},$$

and the intermediate (convex-combination) level $t^{n+\theta} := t_n + \theta\Delta t$, $\theta \in [1/2, 1]$, together with

$$w_h^{n+\theta} := (1 - \theta)w_h^n + \theta w_h^{n+1}, \quad \hat{w}_h^{n+\theta} := (1 - \theta)\hat{w}_h^n + \theta \hat{w}_h^{n+1},$$

for $w \in \{u, v, p, q\}$.

5.1. Fully discrete HDG scheme. Given $(u_h^n, v_h^n, p_h^n, q_h^n)$ and $(\hat{u}_h^n, \hat{v}_h^n, \hat{q}_h^n)$ at time t_n , we compute $(u_h^{n+1}, v_h^{n+1}, p_h^{n+1}, q_h^{n+1})$ and $(\hat{u}_h^{n+1}, \hat{v}_h^{n+1}, \hat{q}_h^{n+1})$ by imposing the HDG equations at the intermediate level $n + \theta$ and replacing the time derivative by $\delta_t u_h^{n+1}$. More precisely, we seek

$$(u_h^{n+1}, q_h^{n+1}, p_h^{n+1}, v_h^{n+1}) \in [V_h^k]^4, \quad \hat{u}_h^{n+1} \in M_h(0), \quad \hat{v}_h^{n+1} \in \widetilde{M}_h^R, \quad \hat{q}_h^{n+1} \in \widetilde{M}_h^L,$$

such that for all test functions $(\phi_u, \phi_q, \phi_p, \phi_v) \in [V_h^k]^4$, $\mu_v \in \widetilde{M}_h^R$, $\mu_q \in \widetilde{M}_h^L$, and $\mu_p \in M_h(0)$,

$$\begin{aligned} (\delta_t u_h^{n+1}, \phi_u)_{\mathcal{T}_h} + (p_h^{n+\theta}, \partial_x \phi_u)_{\mathcal{T}_h} - (f(u_h^{n+\theta}), \partial_x \phi_u)_{\mathcal{T}_h} - \gamma(v_h^{n+\theta}, \phi_u)_{\mathcal{T}_h} \\ - \widehat{\langle \hat{p}_h^{n+\theta} - f(u_h^{n+\theta}), \phi_u \rangle}_{\partial \mathcal{T}_h} = 0, \end{aligned} \quad (5.1a)$$

$$-(v_h^{n+\theta}, \partial_x \phi_v)_{\mathcal{T}_h} - (u_h^{n+\theta}, \phi_v)_{\mathcal{T}_h} + \langle \hat{v}_h^{n+\theta}, \phi_v \rangle_{\partial \mathcal{T}_h} = 0, \quad (5.1b)$$

$$(p_h^{n+\theta}, \phi_p)_{\mathcal{T}_h} + \beta(q_h^{n+\theta}, \partial_x \phi_p)_{\mathcal{T}_h} - \beta(\hat{q}_h^{n+\theta}, \phi_p)_{\mathcal{T}_h} = 0, \quad (5.1c)$$

$$(q_h^{n+\theta}, \phi_q)_{\mathcal{T}_h} + (u_h^{n+\theta}, \partial_x \phi_q)_{\mathcal{T}_h} - \langle \hat{u}_h^{n+\theta}, \phi_q \rangle_{\partial \mathcal{T}_h} = 0. \quad (5.1d)$$

The transmission conditions are imposed at time level $n + \theta$:

$$\langle \widehat{v}_h^{n+\theta}, \mu_v n \rangle_{\partial\mathcal{T}_h} = \langle v_R^{n+\theta}, \mu_v n \rangle_{\{x_R\}}, \quad (5.2a)$$

$$\langle \widehat{q}_h^{n+\theta}, \mu_q n \rangle_{\partial\mathcal{T}_h} = \langle q_L^{n+\theta}, \mu_q n \rangle_{\{x_L\}}, \quad (5.2b)$$

$$\langle \widehat{p}_h^{n+\theta} - f(\widehat{u}_h^{n+\theta}), \mu_p n \rangle_{\partial\mathcal{T}_h} = 0, \quad (5.2c)$$

for all $\mu_v \in \widetilde{M}_h^L$, $\mu_q \in \widetilde{M}_h^R$, and $\mu_p \in M_h(0)$. The numerical traces at $n + \theta$ are defined exactly as in the semi-discrete scheme, but evaluated at the intermediate level in I_i :

$$\widehat{v}_h^{n+\theta} = v_h^{n+\theta} + \tau_{vq}(\widehat{q}_h^{n+\theta} - q_h^{n+\theta})n, \quad \text{on } x_{i-1}, \quad (5.3a)$$

$$\widehat{q}_h^{n+\theta} = q_h^{n+\theta} + \tau_{qv}(\widehat{v}_h^{n+\theta} - v_h^{n+\theta})n, \quad \text{on } x_i, \quad (5.3b)$$

$$\widehat{p}_h^{n+\theta} = p_h^{n+\theta} + \tau_{pu}(\widehat{u}_h^{n+\theta} - u_h^{n+\theta})n, \quad \text{on } \partial I_i, \quad (5.3c)$$

$$\widehat{f}(u_h^{n+\theta}) = f(u_h^{n+\theta}) - \tau_f(\widehat{u}_h^{n+\theta} - u_h^{n+\theta})n, \quad \text{on } \partial I_i, \quad (5.3d)$$

and the boundary conditions for each time level can be defined by (3.7). Since $f(u_h^{n+\theta})$ is nonlinear, (5.1)–(5.3) defines a nonlinear system at each time step. In practice we solve it by Newton's method or a damped fixed-point iteration, exploiting the HDG static condensation: for given traces $(\widehat{u}_h^{n+\theta}, \widehat{v}_h^{n+\theta}, \widehat{q}_h^{n+\theta})$, the element unknowns $(u_h^{n+\theta}, v_h^{n+\theta}, p_h^{n+\theta}, q_h^{n+\theta})$ are obtained locally, and the global coupling occurs only through the transmission conditions.

We set $u_h^0 := P u_0$. The remaining fields (v_h^0, p_h^0, q_h^0) and traces can be obtained by solving the local mixed relations $q = u_x$, $p = \beta q_x$, $v_x = u$ which are enforced in the HDG sense (3.3) at $t = 0$ with u_h fixed at u_h^0 .

5.2. Discrete energy stability.

Define the discrete energy

$$E_h^n := \frac{1}{2} \|u_h^n\|_{\mathcal{T}_h}^2.$$

The fully discrete stability proof follows the semi-discrete argument verbatim, except that the time derivative term is handled by the standard θ -identity below.

For any a, b in an inner-product space and $\theta \in [0, 1]$,

$$(b - a, (1 - \theta)a + \theta b) = \frac{1}{2} \left(\|b\|^2 - \|a\|^2 + (2\theta - 1)\|b - a\|^2 \right). \quad (5.4)$$

Theorem 5.1 (Fully discrete stability). *Assume homogeneous boundary data and Assumption 3.1 on the stabilization parameters. Then the fully discrete scheme (5.1)–(5.3) satisfies the energy inequality*

$$E_h^{n+1} - E_h^n + \frac{2\theta - 1}{2} \|u_h^{n+1} - u_h^n\|_{\mathcal{T}_h}^2 + \Delta t \mathcal{D}_h^{n+\theta} \leq 0, \quad \forall n \geq 0,$$

where $\mathcal{D}_h^{n+\theta} \geq 0$ is the same (trace-based) dissipation functional as in the semi-discrete identity (3.10), evaluated at time level $n + \theta$.

Proof. Choosing the test functions:

$$\phi_u = u_h^{n+\theta}, \quad \phi_v = -\gamma v_h^{n+\theta}, \quad \phi_p = -q_h^{n+\theta}, \quad \phi_q = p_h^{n+\theta},$$

in (5.1), adding (5.1a)–(5.1d), and applying the similar algebraic manipulations along with multiple integration by parts and transmission conditions give exactly the semi-discrete energy balance (3.10) at level $n + \theta$, except for the time term $(\delta_t u_h^{n+1}, u_h^{n+\theta})_{\mathcal{T}_h}$:

$$(\delta_t u_h^{n+1}, u_h^{n+\theta})_{\mathcal{T}_h} + \mathcal{D}_h^{n+\theta} = 0.$$

Furthermore, applying identity (5.4) elementwise yields

$$(\delta_t u_h^{n+1}, u_h^{n+\theta})_{\mathcal{T}_h} = \frac{1}{2\Delta t} \left(\|u_h^{n+1}\|_{\mathcal{T}_h}^2 - \|u_h^n\|_{\mathcal{T}_h}^2 + (2\theta - 1)\|u_h^{n+1} - u_h^n\|_{\mathcal{T}_h}^2 \right).$$

A dissipation functional $\mathcal{D}_h^{n+\theta}$ controlled by Assumption 3.1 and the boundary conditions. Since $\theta \geq 1/2$, the extra term $\frac{2\theta-1}{2}\|u_h^{n+1} - u_h^n\|^2$ is nonnegative and the conclusion follows. \square

Remark 5.2 (Role of θ). *The Crank–Nicolson choice $\theta = \frac{1}{2}$ removes the additional time-dissipation term $\frac{2\theta-1}{2} \|u_h^{n+1} - u_h^n\|^2$, making the method the least dissipative in time. For $\theta = 1$ (backward Euler), the method adds numerical dissipation in time.*

5.3. Fully discrete error analysis. We present the fully discrete error analysis for the θ -scheme (5.1)–(5.3). Throughout we assume the stabilization parameters satisfy Assumption 3.1. For any sufficiently smooth scalar function $g(t)$ define the convex combination of its endpoint values

$$g^{n+\theta,*} := (1 - \theta)g(t_n) + \theta g(t_{n+1}),$$

and the intermediate-time mismatch

$$\mu_g^{n+\theta} := g^{n+\theta,*} - g(t^{n+\theta}). \quad (5.5)$$

We also define the time discretization error for u at intermediate step:

$$\eta_u^{n+\theta} := \frac{u(t_{n+1}) - u(t_n)}{\Delta t} - u_t(t^{n+\theta}) =: \delta_t u(t_{n+1}) - u_t(t^{n+\theta}). \quad (5.6)$$

For the nonlinear flux we set

$$\mathcal{M}_f^{n+\theta} := f(u(t^{n+\theta})) - f(u^{n+\theta,*}). \quad (5.7)$$

Write $t_* := t^{n+\theta}$. Using Taylor expansions around t_* ,

$$\begin{aligned} u(t_{n+1}) &= u(t_*) + (1 - \theta)\Delta t u_t(t_*) + \frac{(1 - \theta)^2 \Delta t^2}{2} u_{tt}(\xi_1), \\ u(t_n) &= u(t_*) - \theta \Delta t u_t(t_*) + \frac{\theta^2 \Delta t^2}{2} u_{tt}(\xi_0), \end{aligned}$$

for some $\xi_0, \xi_1 \in (t_n, t_{n+1})$. Subtracting and dividing by Δt gives the explicit structure

$$\eta_u^{n+\theta} = \left(\frac{1}{2} - \theta \right) \Delta t u_{tt}(t_*) + \mathcal{O}(\Delta t^2), \quad (5.8)$$

where the $\mathcal{O}(\Delta t^2)$ term involves u_{ttt} . Therefore, if $\theta \neq \frac{1}{2}$ (in particular $\theta = 1$ backward Euler), the leading term in (5.8) is proportional to $\Delta t u_{tt}$, hence the method is first order in time, and if $\theta = \frac{1}{2}$ (Crank–Nicolson) so $\eta_u^{n+\frac{1}{2}} = \mathcal{O}(\Delta t^2)$ and the method is second order in time. Thus a simple applications of Taylor's theorem proves the following lemma on time bound estimates.

Lemma 5.3 (Time remainder bounds). *Assume $u_{tt} \in L^2(t_n, t_{n+1}; L^2(\Omega))$. Then for any $\theta \in [0, 1]$,*

$$\|\eta_u^{n+\theta}\|_{L^2(\Omega)}^2 \leq C \Delta t \int_{t_n}^{t_{n+1}} \|u_{tt}(t)\|_{L^2(\Omega)}^2 dt, \quad (5.9)$$

$$\|\mu_u^{n+\theta}\|_{L^2(\Omega)}^2 \leq C \Delta t^3 \int_{t_n}^{t_{n+1}} \|u_{tt}(t)\|_{L^2(\Omega)}^2 dt, \quad (5.10)$$

and similarly for $\mu_v^{n+\theta}$, $\mu_p^{n+\theta}$, $\mu_q^{n+\theta}$ under the corresponding time regularity. Moreover, if $\theta = \frac{1}{2}$ and $u_{ttt} \in L^2(t_n, t_{n+1}; L^2(\Omega))$, then

$$\|\eta_u^{n+\frac{1}{2}}\|_{L^2(\Omega)}^2 \leq C \Delta t^3 \int_{t_n}^{t_{n+1}} \|u_{ttt}(t)\|_{L^2(\Omega)}^2 dt. \quad (5.11)$$

If f is locally Lipschitz and u is bounded, then

$$\|\mathcal{M}_f^{n+\theta}\|_{L^2(\Omega)} \leq C \|\mu_u^{n+\theta}\|_{L^2(\Omega)}. \quad (5.12)$$

Define endpoint projection errors and discrete errors (as in the semi-discrete analysis):

$$e_\omega^n := \omega(t_n) - \omega_h^n, \quad e_\omega^n = \xi_\omega^n - \rho_\omega^n, \quad \xi_\omega^n := P\omega(t_n) - \omega_h^n, \quad \rho_\omega^n := P\omega(t_n) - \omega(t_n),$$

for $\omega \in \{u, v, p, q\}$. At the intermediate level we use the convex combinations

$$\xi_\omega^{n+\theta} := (1 - \theta)\xi_\omega^n + \theta\xi_\omega^{n+1}, \quad \rho_\omega^{n+\theta} := (1 - \theta)\rho_\omega^n + \theta\rho_\omega^{n+1}.$$

On the skeleton, define the intermediate-level trace errors using the same convex-combination reference values:

$$\widehat{\xi}_u^{n+\theta} := u^{n+\theta,*} - \widehat{u}_h^{n+\theta}, \quad \widehat{\xi}_v^{n+\theta} := v^{n+\theta,*} - \widehat{v}_h^{n+\theta}, \quad \widehat{\xi}_q^{n+\theta} := q^{n+\theta,*} - \widehat{q}_h^{n+\theta}, \quad \widehat{\xi}_p^{n+\theta} := p^{n+\theta,*} - \widehat{p}_h^{n+\theta}. \quad (5.13)$$

(Here $\widehat{v}_h^{n+\theta}, \widehat{q}_h^{n+\theta}, \widehat{p}_h^{n+\theta}$ are the numerical traces defined by (5.3).) Exactly as in (4.5)–(4.7) of the semi-discrete analysis, the trace definitions imply the identities

$$\widehat{\xi}_v^{n+\theta} = \xi_v^{n+\theta} + \tau_{vq}(\widehat{\xi}_q^{n+\theta} - \xi_q^{n+\theta})n - (\rho_v^{n+\theta} - \tau_{vq}\rho_q^{n+\theta}n), \quad \text{at } x_{i-1}, \quad (5.14)$$

$$\widehat{\xi}_q^{n+\theta} = \xi_q^{n+\theta} + \tau_{qv}(\widehat{\xi}_v^{n+\theta} - \xi_v^{n+\theta})n - (\rho_q^{n+\theta} - \tau_{qv}\rho_v^{n+\theta}n), \quad \text{at } x_i, \quad (5.15)$$

$$\widehat{\xi}_p^{n+\theta} = \xi_p^{n+\theta} + \tau_{pu}(\widehat{\xi}_u^{n+\theta} - \xi_u^{n+\theta})n - (\rho_p^{n+\theta} - \tau_{pu}\rho_u^{n+\theta}n), \quad \text{on } \partial I_i. \quad (5.16)$$

Let $\phi_u, \phi_v, \phi_p, \phi_q \in V_h^k$ be arbitrary. Subtracting the fully discrete scheme (5.1) (evaluated at $t^{n+\theta}$) from the exact weak identities at time $t^{n+\theta}$ and rewriting all exact quantities in terms of $(\cdot)^{n+\theta,*}$ plus the remainders (5.5)–(5.7) yields the following system:

$$\begin{aligned} & (\delta_t \xi_u^{n+1}, \phi_u)_{\mathcal{T}_h} + (\xi_p^{n+\theta}, \partial_x \phi_u)_{\mathcal{T}_h} - (f(u^{n+\theta,*}) - f(u_h^{n+\theta}), \partial_x \phi_u)_{\mathcal{T}_h} - \gamma(\xi_v^{n+\theta}, \phi_u)_{\mathcal{T}_h} \\ & \quad - \langle \widehat{\xi}_p^{n+\theta}, \phi_u n \rangle_{\partial \mathcal{T}_h} + \langle f(u^{n+\theta,*}) - f(\widehat{u}_h^{n+\theta}), \phi_u n \rangle_{\partial \mathcal{T}_h} = \mathcal{R}_u^{n+\theta}(\phi_u), \end{aligned} \quad (5.17a)$$

$$-(\xi_v^{n+\theta}, \partial_x \phi_v)_{\mathcal{T}_h} - (\xi_u^{n+\theta}, \phi_v)_{\mathcal{T}_h} + \langle \widehat{\xi}_v^{n+\theta}, \phi_v n \rangle_{\partial \mathcal{T}_h} = \mathcal{R}_v^{n+\theta}(\phi_v), \quad (5.17b)$$

$$(\xi_p^{n+\theta}, \phi_p)_{\mathcal{T}_h} + \beta(\xi_q^{n+\theta}, \partial_x \phi_p)_{\mathcal{T}_h} - \beta \langle \widehat{\xi}_q^{n+\theta}, \phi_p n \rangle_{\partial \mathcal{T}_h} = \mathcal{R}_p^{n+\theta}(\phi_p), \quad (5.17c)$$

$$(\xi_q^{n+\theta}, \phi_q)_{\mathcal{T}_h} + (\xi_u^{n+\theta}, \partial_x \phi_q)_{\mathcal{T}_h} - \langle \widehat{\xi}_u^{n+\theta}, \phi_q n \rangle_{\partial \mathcal{T}_h} = \mathcal{R}_q^{n+\theta}(\phi_q), \quad (5.17d)$$

where the remainder functionals are fully explicit:

$$\begin{aligned} \mathcal{R}_u^{n+\theta}(\phi_u) := & (\eta_u^{n+\theta}, \phi_u)_{\mathcal{T}_h} + (\mu_p^{n+\theta}, \partial_x \phi_u)_{\mathcal{T}_h} + (\mathcal{M}_f^{n+\theta}, \partial_x \phi_u)_{\mathcal{T}_h} - \gamma(\mu_v^{n+\theta}, \phi_u)_{\mathcal{T}_h} \\ & - \langle \mu_p^{n+\theta} + \mathcal{M}_f^{n+\theta}, \phi_u n \rangle_{\partial \mathcal{T}_h}, \end{aligned} \quad (5.18a)$$

$$\mathcal{R}_v^{n+\theta}(\phi_v) := -(\mu_v^{n+\theta}, \partial_x \phi_v)_{\mathcal{T}_h} - (\mu_u^{n+\theta}, \phi_v)_{\mathcal{T}_h} + \langle \mu_v^{n+\theta}, \phi_v n \rangle_{\partial \mathcal{T}_h}, \quad (5.18b)$$

$$\mathcal{R}_p^{n+\theta}(\phi_p) := -(\mu_p^{n+\theta}, \phi_p)_{\mathcal{T}_h} - \beta(\mu_q^{n+\theta}, \partial_x \phi_p)_{\mathcal{T}_h} + \beta \langle \mu_q^{n+\theta}, \phi_p n \rangle_{\partial \mathcal{T}_h}, \quad (5.18c)$$

$$\mathcal{R}_q^{n+\theta}(\phi_q) := -(\mu_q^{n+\theta}, \phi_q)_{\mathcal{T}_h} - (\mu_u^{n+\theta}, \partial_x \phi_q)_{\mathcal{T}_h} + \langle \mu_u^{n+\theta}, \phi_q n \rangle_{\partial \mathcal{T}_h}. \quad (5.18d)$$

where we have used

$$\begin{aligned} (u_t(t^{n+\theta}), \phi_u)_{\mathcal{T}_h} - (\delta_t u_h^{n+1}, \phi_u)_{\mathcal{T}_h} &= (\delta_t u(t_{n+1}), \phi_u)_{\mathcal{T}_h} - (\eta_u^{n+\theta}, \phi_u)_{\mathcal{T}_h} - (\delta_t u_h^{n+1}, \phi_u)_{\mathcal{T}_h} \\ &= (\delta_t \xi_u^{n+1}, \phi_u)_{\mathcal{T}_h} - (\eta_u^{n+\theta}, \phi_u)_{\mathcal{T}_h}, \end{aligned}$$

since P is the L^2 -projection onto V_h^k , for any $\phi_u \in V_h^k$, we have $(\delta_t P u(t_{n+1}), \phi_u) = (\delta_t u(t_{n+1}), \phi_u)$, similarly for other variable. Under homogeneous boundary data, the transmission conditions yield the same relations as in the semi-discrete case:

$$\langle \widehat{\xi}_v^{n+\theta}, \mu_v n \rangle_{\partial \mathcal{T}_h} = 0, \quad \forall \mu_v \in \widetilde{M}_h^R, \quad (5.19a)$$

$$\langle \widehat{\xi}_q^{n+\theta}, \mu_q n \rangle_{\partial \mathcal{T}_h} = 0, \quad \forall \mu_q \in \widetilde{M}_h^L, \quad (5.19b)$$

$$\langle \widehat{\xi}_p^{n+\theta} - (f(u^{n+\theta,*}) - f(\widehat{u}_h^{n+\theta})), \mu_p n \rangle_{\partial \mathcal{T}_h} = 0, \quad \forall \mu_p \in M_h(0). \quad (5.19c)$$

Choose the similar test functions as in the semi-discrete error proof of Theorem 4.3, now at level $n + \theta$:

$$\phi_u = \xi_u^{n+\theta}, \quad \phi_v = -\gamma \xi_v^{n+\theta}, \quad \phi_p = -\xi_q^{n+\theta}, \quad \phi_q = \xi_p^{n+\theta}.$$

Add (5.17a)–(5.17d) and use the same algebraic manipulations, integration-by-parts, and transmission-condition arguments as in the semi-discrete case to obtain the discrete error energy identity, with

N_e	$k = 1$		$k = 2$		$k = 3$	
	error	rate	error	rate	error	rate
$\theta = \frac{1}{2}$ (Crank–Nicolson), $\Delta t = 0.001$						
2	8.022×10^{-1}	–	6.661×10^{-2}	–	3.427×10^{-2}	–
4	1.355×10^{-1}	2.565	1.671×10^{-2}	1.995	1.406×10^{-3}	4.607
8	3.013×10^{-2}	2.169	1.765×10^{-3}	3.243	8.572×10^{-5}	4.036
16	6.907×10^{-3}	2.125	2.152×10^{-4}	3.036	5.340×10^{-6}	4.005
32	1.670×10^{-3}	2.048	2.680×10^{-5}	3.006	3.658×10^{-7}	3.868
$\theta = 1$ (backward Euler), $\Delta t = 0.1 h^{k+1}$						
2	7.375×10^{-1}	–	5.471×10^{-2}	–	1.083×10^{-1}	–
4	1.293×10^{-1}	2.512	1.784×10^{-2}	1.617	1.740×10^{-2}	2.638
8	2.920×10^{-2}	2.147	2.270×10^{-3}	2.975	1.237×10^{-3}	3.814
16	6.788×10^{-3}	2.105	2.895×10^{-4}	2.971	7.787×10^{-5}	3.990

TABLE 1. Convergence test at $T = 0.5$ with $(\alpha, \beta, \gamma = (1, 0.5, 1))$. We report the L^2 error in u and the observed rate for polynomial degrees $k = 1, 2, 3$.

the only new step being the time term:

$$(\delta_t \xi_u^{n+1}, \xi_u^{n+\theta})_{\mathcal{T}_h} = \frac{1}{2\Delta t} \left(\|\xi_u^{n+1}\|_{\mathcal{T}_h}^2 - \|\xi_u^n\|_{\mathcal{T}_h}^2 + (2\theta - 1) \|\xi_u^{n+1} - \xi_u^n\|_{\mathcal{T}_h}^2 \right) \quad (\text{by (5.4)}).$$

The right-hand side contributions are exactly the remainder functionals (5.18) tested with the chosen test functions and are bounded using Cauchy–Schwarz and Young’s inequality together with Lemma 5.3 and the spatial projection estimates from the semi-discrete analysis. Summing over n and applying a discrete Gronwall inequality and combining with the spatial estimate from the semi-discrete analysis (order $h^{k+\frac{1}{2}}$) finally gives

$$\max_{0 \leq n \leq N} \|u(t_n) - u_h^n\|_{L^2(\Omega)} \leq C \left(h^{k+\frac{1}{2}} + \Delta t^r \right), \quad r = \begin{cases} 1, & \theta \neq \frac{1}{2} \text{ (e.g. backward Euler } \theta = 1\text{),} \\ 2, & \theta = \frac{1}{2} \text{ (Crank–Nicolson),} \end{cases}$$

under the corresponding time regularity assumed in Lemma 5.3.

6. NUMERICAL EXAMPLES

We now present two numerical examples to verify the convergence of the proposed HDG method. In following examples, the stabilization parameters are chosen according to Assumption 3.1. In particular, we use the (constant) stabilization parameters

$$\tau_{pu} = 2, \quad \tau_{vq} = 0.9\sqrt{\beta/\gamma}, \quad \tau_{qv} = 0.9\sqrt{\gamma/\beta}, \quad \tau_f = 2.$$

Example 6.1. Smooth manufactured solution (Accuracy test). We assess the spatial accuracy of the proposed HDG scheme using a smooth manufactured solution on $\Omega = (0, 2\pi)$ with parameters $\beta = 0.5$ and $\gamma = 1$. We prescribe the exact solution

$$u(x, t) = e^{-t} \sin(x), \quad t \in [0, T], \quad T = 0.5.$$

The source term $g(x, t)$ is chosen so that (u, v) satisfies the Ostrovsky system (1.1). We impose boundary data consistent with the manufactured solution.

For time integration we use the θ -scheme with $\theta = \frac{1}{2}$ (Crank–Nicolson) and $\theta = 1$ (backward Euler implicit) with fixed time steps $\Delta t = 0.001$ and $\Delta t = 0.1 h^{k+1}$ respectively, chosen sufficiently small so that the temporal error does not dominate the spatial error on the meshes considered. For each polynomial degree $k \in \{1, 2, 3\}$ we compute the numerical solution at $T = 0.5$. Although Theorem 4.3 guarantees an $O(h^{k+1/2})$ bound in $L^2(\Omega)$, the observed rates in Table 1 are closer to $k + 1$. This behavior is consistent with the commonly observed superconvergent behavior of hybridized methods in practice.

Example 6.2. Periodic solitary-wave propagation (numerical profile). We test whether the proposed HDG scheme (3.3)–(3.6) propagates a localized solitary-wave profile on a large periodic domain without spurious distortion.

We consider the Ostrovsky equation (1.1) in the mixed first-order form (3.1) on the periodic interval $\Omega = (0, L)$ with $L \gg 1$. Since $v_x = u$ determines v only up to an additive constant, we fix the gauge by prescribing the mean-zero compatibility

$$\int_0^L u(x, t) dx = 0, \quad (6.1)$$

so that the periodic anti-derivative (generalized inverse) ∂_x^{-1} is well-defined on mean-zero functions and v is uniquely determined once a reference value (e.g. $v(0, t) = 0$) is chosen.

A solitary traveling wave is a coherent structure of the form

$$u(x, t) = U(\xi), \quad \xi = x - c_w t, \quad (6.2)$$

where U is localized on \mathbb{R} and, on a sufficiently large periodic box, is exponentially small near $x = 0$ and $x = L$. From (3.1) we have $q = U'$, $p = \beta U''$, and $v_x = u$ implies $v(\xi) = \partial_\xi^{-1} U(\xi)$, interpreted as the mean-zero periodic anti-derivative consistent with (6.1). Substituting (6.2) into the last equation of (3.1) yields

$$-c_w U' - \beta U''' + (f(U))' - \gamma \partial_\xi^{-1} U = 0. \quad (6.3)$$

Integrating once in ξ and using the mean-zero periodic convention (so the integration constant is zero) gives the stationary profile equation

$$-c_w U - \beta U'' + f(U) - \gamma \partial_\xi^{-2} U = 0, \quad \widehat{U}(0) = 0, \quad (6.4)$$

where ∂_ξ^{-2} denotes the periodic inverse of ∂_ξ^2 acting on mean-zero functions.

Let $\widehat{U}(\kappa)$ denote the Fourier coefficients on $(0, L)$ with wave numbers $\kappa = \frac{2\pi}{L} m$, $m \in \mathbb{Z}$. Taking Fourier transforms in (6.4) yields, for $\kappa \neq 0$,

$$\left(\beta \kappa^2 - c_w + \frac{\gamma}{\kappa^2} \right) \widehat{U}(\kappa) + \widehat{f(U)}(\kappa) = 0, \quad \widehat{U}(0) = 0. \quad (6.5)$$

Thus the nonzero modes satisfy the nonlinear fixed-point map

$$\widehat{U}(\kappa) = -\frac{\widehat{f(U)}(\kappa)}{\beta \kappa^2 - c_w + \gamma/\kappa^2}, \quad \kappa \neq 0, \quad \widehat{U}(0) = 0. \quad (6.6)$$

In our computations we take $f(u) = \frac{\alpha}{2} u^2$ and construct a numerical profile by a stabilized (Petviashvili-type) fixed-point iteration [12]. Given an iterate $U^{(n)}$, we compute $F^{(n)} = \frac{\alpha}{2} (U^{(n)})^2$, evaluate its Fourier coefficients $\widehat{F^{(n)}}$ by FFT, and update for $\kappa \neq 0$ by

$$\widehat{U}^{(n+1)}(\kappa) = -M_n^p \frac{\widehat{F^{(n)}}(\kappa)}{\beta \kappa^2 - c_w + \gamma/\kappa^2}, \quad \widehat{U}^{(n+1)}(0) = 0, \quad (6.7)$$

where M_n is an amplitude-correction factor and $p > 0$ is an exponent suitable for quadratic nonlinearities. We apply mild relaxation $U^{(n+1)} \leftarrow (1 - \omega)U^{(n)} + \omega U^{(n+1)}$ with $\omega \in (0, 1]$, and enforce the mean-zero constraint by subtracting the spatial average after each iterate. For the quadratic nonlinearity we take the Petviashvili exponent $p = 2$ and use relaxation $\omega = 0.8$. We iterate until the residual of (6.5) is below a prescribed tolerance. On a large box, the resulting periodic profile satisfies $|U(0)| \approx |U(L)| \ll 1$, i.e. the tails are negligible at the endpoints.

We take the computed profile as initial data $u_0(x) = U(x - x_0)$ (shifted so the peak is away from the boundaries) and initialize $q_0 = u_{0x}$, $p_0 = \beta u_{0xx}$, and $v_0 = \partial_x^{-1} u_0$ using the same periodic mean-zero convention (6.1).

To assess shape preservation, we compare the HDG solution $u_h(x, t)$ with the traveling-wave reference obtained by periodic translation of the numerical profile:

$$u_{\text{ref}}(x, t) := U(x - c_w t). \quad (6.8)$$

This u_{ref} is not an exact solution of the full PDE on a finite periodic box, but it is the appropriate benchmark for short-time propagation.

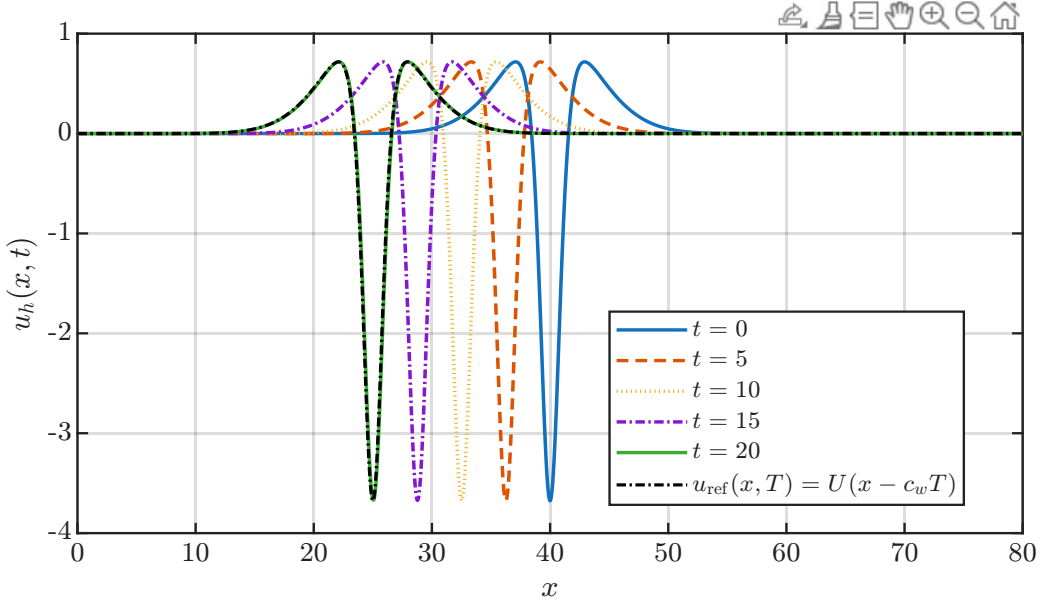


FIGURE 1. Solitary-wave propagation with $N_e = 256$, $k = 2$, $\Delta t = 0.05$, $T = 20$. Shown are $u_h(\cdot, t)$ at $t = 0, 5, 10, 15, 20$ and the translated reference $u_{\text{ref}}(\cdot, T) = U(\cdot - c_w T)$.

In this experiment we take $\alpha = 2$, $\beta = 1$, $\gamma = \frac{1}{4}$, $L = 80$ (periodic), and wave speed $c_w = -0.75$ (which lies in the regime $c_w < 2\sqrt{\beta\gamma}$ considered in the reference setup). We compute the numerical profile on a Fourier grid of $K = 512$ points and then evolve the HDG scheme on a mesh of N_e elements with polynomial degree k and a Crank–Nicolson time discretization ($\theta = \frac{1}{2}$).

Figure 1 shows snapshots of $u_h(x, t)$ at times $t = 0, 5, 10, 15, 20$, together with the translated reference profile $u_{\text{ref}}(x, T)$ at the final time. We observe that the wave translates to the right/left according to the sign of c_w and remains localized, with only mild dispersive radiation, indicating that the HDG discretization captures coherent travelling-wave dynamics of the Ostrovsky model.

Solitary waves in the Ostrovsky model (1.1) represent long, weakly nonlinear dispersive waves in a rotating medium (e.g. internal waves under the Coriolis effect). They arise from a balance of nonlinearity and dispersion modified by rotation, producing a coherent structure that propagates over long times with a nearly unchanged shape. The present experiment verifies that the HDG discretization reproduces this qualitative behaviour and provides a practical benchmark for tracking numerical dispersion and dissipation [9, 12, 37].

Example 6.3. Peakon solution and the singular limit. We illustrate a non-smooth benchmark and the singular regime $\beta \rightarrow 0$, where the Ostrovsky equation (1.1) converges to the Ostrovsky–Hunter (OH) equation; see, e.g., [7].

Following [52, Example 4.3], we take the “peakon”

$$u_0(x) = \begin{cases} \frac{1}{6} \left(x - \frac{1}{2} \right)^2 + \frac{1}{6} \left(x - \frac{1}{2} \right) + \frac{1}{36}, & x \in \left[0, \frac{1}{2} \right], \\ \frac{1}{6} \left(x - \frac{1}{2} \right)^2 - \frac{1}{6} \left(x - \frac{1}{2} \right) + \frac{1}{36}, & x \in \left[\frac{1}{2}, 1 \right], \end{cases} \quad u_0(x+1) = u_0(x). \quad (6.9)$$

For the OH case ($\beta = 0$), this yields the explicit traveling-wave solution

$$u(x, t) = u_0 \left(x - \frac{t}{36} \right), \quad (6.10)$$

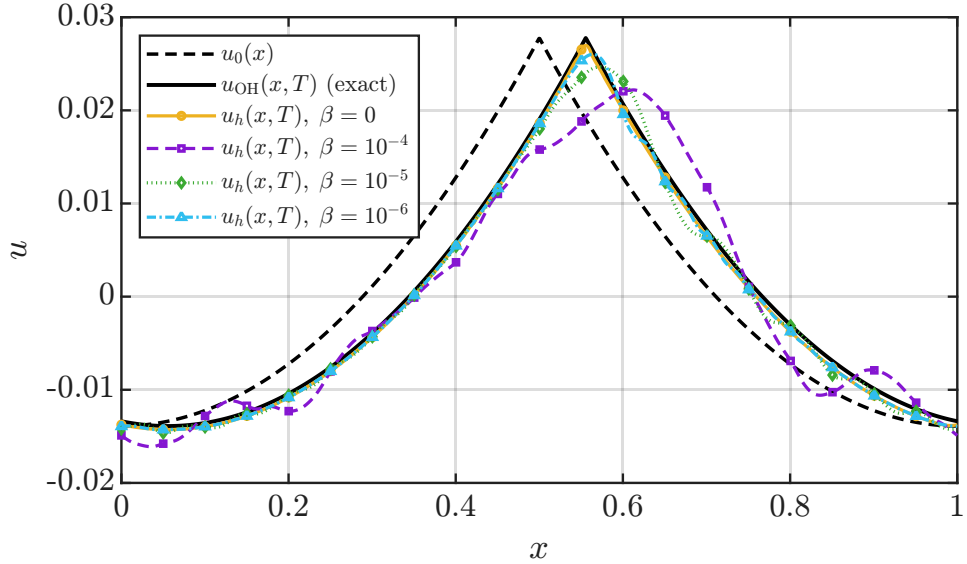


FIGURE 2. Peakon solution and the limit $\beta \rightarrow 0$. Shown are the initial condition u_0 from (6.9), the OH reference profile $u_{\text{OH}}(\cdot, T)$ given by (6.10), and periodic HDG solutions $u_h(\cdot, T)$ for several values of β .

so the profile translates at speed $c = \frac{1}{36}$ and returns to u_0 at times $T \in 36\mathbb{N}$. To initialize the mixed variables in (3.1) we set $q(\cdot, 0) = \partial_x u_0$, $v(\cdot, 0) = \int_0^x u_0(s) ds$ (hence $v(0, 0) = 0$ and this is the periodic mean-zero antiderivative gauge), and $p(\cdot, 0) = \beta \partial_x q(\cdot, 0)$.

The Ostrovsky equation models weakly nonlinear long waves in a rotating fluid; the term involving γ encodes the large-scale restoring (Coriolis) effect, while β controls dispersive regularization [7, 8]. The peakon-type profile (6.9) represents a coherent structure with a sharp corner (discontinuous slope), making it a demanding benchmark for high-order methods.

We fix $\alpha = 1$ and $\gamma = 1$ and compute periodic HDG solutions for a sequence $\beta \in \{0, \beta_1, \beta_2, \dots\}$ with $\beta_j \rightarrow 0$. For $\beta = 0$ we validate against the explicit wave (6.10). For $\beta > 0$ we quantify the singular-limit behavior by comparing the OV solution to the OH reference profile at the same final time $T = 2$. We used polynomial degree $k = 2$, elements $N_e = 32$, time step $\Delta t = 0.005$, $\theta = \frac{1}{2}$, and $\beta \in \{0, 10^{-4}, 10^{-5}, 10^{-6}\}$.

Figure 2 shows the initial profile u_0 , the OH reference profile at time T , and the HDG approximations for several values of β . As β decreases, the numerical Ostrovsky curves approach the OH reference, indicating that the proposed HDG method captures the singular limit while accurately transporting a corner-type coherent structure.

7. CONCLUSION

We developed a HDG method for the Ostrovsky equation on a bounded interval by localizing the nonlocal term through the auxiliary variable v defined by $v_x = u$ with a fixed boundary constraint to ensure uniqueness. The resulting formulation admits elementwise elimination of interior unknowns and a global system posed only in terms of numerical traces. For $\beta \neq 0$ and $\gamma > 0$ (under the stated stabilization conditions), we established an L^2 -stability estimate and proved an *a priori* L^2 -error bound for the primary variable u . Numerical experiments confirm the predicted convergence for smooth solutions and demonstrate that the method remains accurate and stable in challenging regimes, including near non-smooth peaked profiles for reduced OH model whenever $\beta \rightarrow 0$. The present HDG design extends naturally to KP-type models [22] in two space dimensions in which the transverse term appears as $\partial_x^{-1} u_{yy}$: one introduces auxiliary variables for y -derivatives (e.g. $w = u_y$, $r = w_y$) and enforces the inverse- x operator through a mixed constraint $v_x = r$ together with an appropriate gauge condition.

DECLARATIONS

Data availability. All numerical experiments can be reproduced from the implementation used in this work. The data supporting the findings of this study are available in the accompanying public repository [41].

Competing interests. The authors declare that they have no competing interests.

Funding. This work has been supported by the Deutsche Forschungsgemeinschaft (DFG, German Research Foundation) – 577175348.

REFERENCES

- [1] G.-Y. Chen and J. P. Boyd. Analytical and numerical studies of weakly nonlocal solitary waves of the rotation-modified Korteweg–de Vries equation. *Physica D: Nonlinear Phenomena*, 155(3-4):201–222, 2001.
- [2] H. Chen, W. Qiu, K. Shi, and M. Solano. A superconvergent HDG method for the Maxwell equations. *Journal of Scientific Computing*, 70:1010–1029, 2017.
- [3] Y. Chen, B. Cockburn, and B. Dong. Superconvergent HDG methods for linear, stationary, third-order equations in one space dimension. *Mathematics of Computation*, 85(302):2715–2742, 2016.
- [4] Y. Chen, B. Dong, and J. Jiang. Optimally convergent hybridizable discontinuous Galerkin method for fifth-order Korteweg–de Vries type equations. *ESAIM: Mathematical Modelling and Numerical Analysis*, 52(6):2283–2306, 2018.
- [5] P. G. Ciarlet. *The finite element method for elliptic problems*, volume 4 of *Studies in Mathematics and its Applications*. North-Holland Publishing Co., Amsterdam-New York-Oxford, 1978.
- [6] B. Cockburn, J. Gopalakrishnan, and R. Lazarov. Unified hybridization of discontinuous Galerkin, mixed, and continuous Galerkin methods for second-order elliptic problems. *SIAM Journal on Numerical Analysis*, 47(2):1319–1365, 2009.
- [7] G. M. Coclite and L. di Ruvo. Convergence of the Ostrovsky equation to the Ostrovsky–Hunter one. *Journal of Differential Equations*, 256(9):3245–3277, 2014.
- [8] G. M. Coclite and L. di Ruvo. Dispersive and diffusive limits for Ostrovsky–Hunter type equations. *NoDEA. Nonlinear Differential Equations and Applications*, 22(6):1733–1763, 2015.
- [9] G. M. Coclite and L. di Ruvo. On the solutions for an Ostrovsky type equation. *Nonlinear Analysis: Real World Applications*, 55:103141, 2020.
- [10] G. M. Coclite, J. Ridder, and N. Risebro. A convergent finite difference scheme for the Ostrovsky–Hunter equation on a bounded domain. *BIT Numerical Mathematics*, 57(1):93–122, 2017.
- [11] B. Dong. Optimally convergent HDG method for third-order Korteweg–de Vries type equations. *Journal of Scientific Computing*, 73(2–3):712–735, 2017.
- [12] Á. Durán. On the Numerical Approximation to Generalized Ostrovsky Equations: I: A Numerical Method and Computation of Solitary-Wave Solutions. In *Nonlinear Systems, Vol. 1: Mathematical Theory and Computational Methods*, pages 339–368. Springer, 2018.
- [13] M. Dwivedi, R. Gutendorf, and A. Rupp. A Hybridizable Discontinuous Galerkin Method for the non-local Camassa–Holm–Kadomtsev–Petviashvili equation. *arXiv preprint arXiv:2601.13800*, 2026.
- [14] M. Dwivedi and T. Sarkar. Convergence of a Conservative Crank–Nicolson Finite Difference Scheme for the KdV Equation. *Mathematical Methods in the Applied Sciences*, 48(17):15602–15619, 2025.
- [15] M. Dwivedi and T. Sarkar. Analysis of a Fully Discrete Local Discontinuous Galerkin Scheme for the Fractional Korteweg–de Vries Equation. *Communications on Applied Mathematics and Computation*, pages 1–44, 2026.
- [16] R. H. Grimshaw, J.-M. He, and L. Ostrovsky. Terminal damping of a solitary wave due to radiation in rotational systems. *Studies in Applied Mathematics*, 101(2):197–210, 1998.
- [17] R. H. Grimshaw, K. Helfrich, and E. R. Johnson. The reduced Ostrovsky equation: Integrability and breaking. *Studies in Applied Mathematics*, 129(4):414–436, 2012.
- [18] G. Gui and Y. Liu. On the Cauchy problem for the Ostrovsky equation with positive dispersion. *Communications in Partial Differential Equations*, 32(12):1895–1916, 2007.
- [19] F. Han and Y. Gao. Spectral stability of constrained solitary waves for a generalized Ostrovsky equation. *Proceedings of the Royal Society of Edinburgh Section A: Mathematics*, pages 1–32, 2024.
- [20] H. Holden, K. H. Karlsen, and N. H. Risebro. Operator splitting methods for generalized Korteweg–de Vries equations. *Journal of Computational Physics*, 153(1):203–222, 1999.
- [21] J. K. Hunter. Numerical solutions of some nonlinear dispersive wave equations. In *Computational solution of nonlinear systems of equations (Fort Collins, CO, 1988)*, volume 26 of *Lectures in Appl. Math.*, pages 301–316. Amer. Math. Soc., Providence, RI, 1990.
- [22] B. B. Kadomtsev and V. I. Petviashvili. On the stability of solitary waves in weakly dispersing media. *Soviet Physics Doklady*, 15:539–541, 1970.
- [23] S. Kawai, S. Sato, and T. Matsuo. Mathematical analysis of a norm-conservative numerical scheme for the Ostrovsky equation. *Japan Journal of Industrial and Applied Mathematics*, 42(1):153–176, 2025.

- [24] C. E. Kenig, G. Ponce, and L. Vega. Well-posedness of the initial value problem for the Korteweg-de Vries equation. *Journal of the American Mathematical Society*, 4(2):323–347, 1991.
- [25] S. Levandovsky and Y. Liu. Stability of solitary waves of a generalized Ostrovsky equation. *SIAM Journal on Mathematical Analysis*, 38(3):985–1011, 2006.
- [26] S. Levandovsky and Y. Liu. Stability and weak rotation limit of solitary waves of the Ostrovsky equation. *Discrete and Continuous Dynamical Systems. Series B*, 7(4):793, 2007.
- [27] F. Linares and A. Milánés. Local and global well-posedness for the Ostrovsky equation. *Journal of Differential Equations*, 222(2):325–340, 2006.
- [28] H. Liu and J. Yan. A local discontinuous Galerkin method for the Korteweg–de Vries equation with boundary effect. *Journal of Computational Physics*, 215(1):197–218, 2006.
- [29] Y. Liu. On the stability of solitary waves for the Ostrovsky equation. *Quarterly of Applied Mathematics*, 65(3):571–589, 2007.
- [30] Y. Liu, D. Pelinovsky, and A. Sakovich. Wave breaking in the Ostrovsky–Hunter equation. *SIAM Journal on Mathematical Analysis*, 42(5):1967–1985, 2010.
- [31] Y. Liu and V. Varlamov. Stability of solitary waves and weak rotation limit for the ostrovsky equation. *Journal of Differential Equations*, 203(1):159–183, 2004.
- [32] P. Lu, R. Maier, and A. Rupp. A localized orthogonal decomposition strategy for hybrid discontinuous Galerkin methods. *ESAIM. Mathematical Modelling and Numerical Analysis*, 59(2):1213–1237, 2025.
- [33] P. Lu, A. Rupp, and G. Kanschat. Homogeneous multigrid for HDG. *IMA Journal of Numerical Analysis*, 42(4):3135–3153, 2022.
- [34] Y. Miyatake, T. Yaguchi, and T. Matsuo. Numerical integration of the ostrovsky equation based on its geometric structures. *Journal of Computational Physics*, 231:4542–4559, 2012.
- [35] M. Musch, A. Rupp, V. Aizinger, and P. Knabner. Hybridizable discontinuous Galerkin method with mixed-order spaces for non-linear diffusion equations with internal jumps. *GEM. International Journal on Geomathematics*, 14(1):Paper No. 18, 25, 2023.
- [36] I. Oikawa. A hybridized discontinuous Galerkin method with reduced stabilization. *Journal of Scientific Computing*, 65(1):327–340, 2015.
- [37] L. Ostrovsky. Nonlinear internal waves in a rotating ocean. *Oceanology*, 18:119–125, 1978.
- [38] J. Peraire, N. C. Nguyen, and B. Cockburn. A hybridizable discontinuous Galerkin method for the compressible Euler and Navier–Stokes equations. Technical Report AIAA-2010-363, American Institute of Aeronautics and Astronautics, 2010. 48th AIAA Aerospace Sciences Meeting, Orlando, FL.
- [39] L. G. Redekopp. Nonlinear waves in geophysics: Long internal waves. *Dynamics in Astrophysics and Geophysics*, 20:59, 1983.
- [40] J. Ridder and A. M. Ruf. A convergent finite difference scheme for the Ostrovsky–Hunter equation with Dirichlet boundary conditions. *BIT Numerical Mathematics*, 59(3):775–796, 2019.
- [41] A. Rupp. *hdg.ostrovsky*: Hybridizable discontinuous Galerkin discretization of the Ostrovsky equation by Mukul Dwivedi in MATLAB. https://github.com/AndreasRupp/hdg_ostrovsky, 2026. GitHub repository.
- [42] A. Samii, N. Panda, C. Michoski, and C. Dawson. A hybridized discontinuous Galerkin method for the nonlinear Korteweg–de Vries equation. *Journal of Scientific Computing*, 68(1):191–212, 2016.
- [43] S. Sato. Geometric numerical integration of the Ostrovsky equation via scalar auxiliary variable approach. *Japan Journal of Industrial and Applied Mathematics*, pages 1–22, 2025.
- [44] V. Vakhnenko. Solitons in a nonlinear model medium. *Journal of Physics A: Mathematical and General*, 25(15):4181, 1992.
- [45] V. Vakhnenko and E. Parkes. The two loop soliton solution of the Vakhnenko equation. *Nonlinearity*, 11(6):1457, 1998.
- [46] J. Wang, Y. Huang, and W. Qiu. An HDG method for linear elasticity with strong symmetric stresses. *Mathematics of Computation*, 88(319):2269–2294, 2019.
- [47] J. Wang and W. Yan. The Cauchy problem for quadratic and cubic Ostrovsky equation with negative dispersion. *Nonlinear Analysis: Real World Applications*, 43:283–307, 2018.
- [48] Y. Xu and C.-W. Shu. Error estimates of the semi-discrete local discontinuous Galerkin method for nonlinear convection–diffusion and KdV equations. *Computer Methods in Applied Mechanics and Engineering*, 196:3805–3822, 2007.
- [49] T. Yaguchi, T. Matsuo, and M. Sugihara. Conservative numerical schemes for the Ostrovsky equation. *Journal of Computational and Applied Mathematics*, 234(4):1036–1048, 2010.
- [50] W. Yan, Y. Li, J. Huang, and J. Duan. The Cauchy problem for the Ostrovsky equation with positive dispersion. *Nonlinear Differential Equations and Applications NoDEA*, 25(3):22, 2018.
- [51] W. Yan, M. Yang, and J. Duan. White noise driven Ostrovsky equation. *Journal of Differential Equations*, 267(10):5701–5735, 2019.
- [52] Q. Zhang and Y. Xia. Discontinuous Galerkin Methods for the Ostrovsky–Vakhnenko Equation. *Journal of Scientific Computing*, 82(2):24, 2020.

DEPARTMENT OF MATHEMATICS, SAARLAND UNIVERSITY, SAARBRÜCKEN, GERMANY

Email address: {mukul.dwivedi;andreas.rupp}@uni-saarland.de